


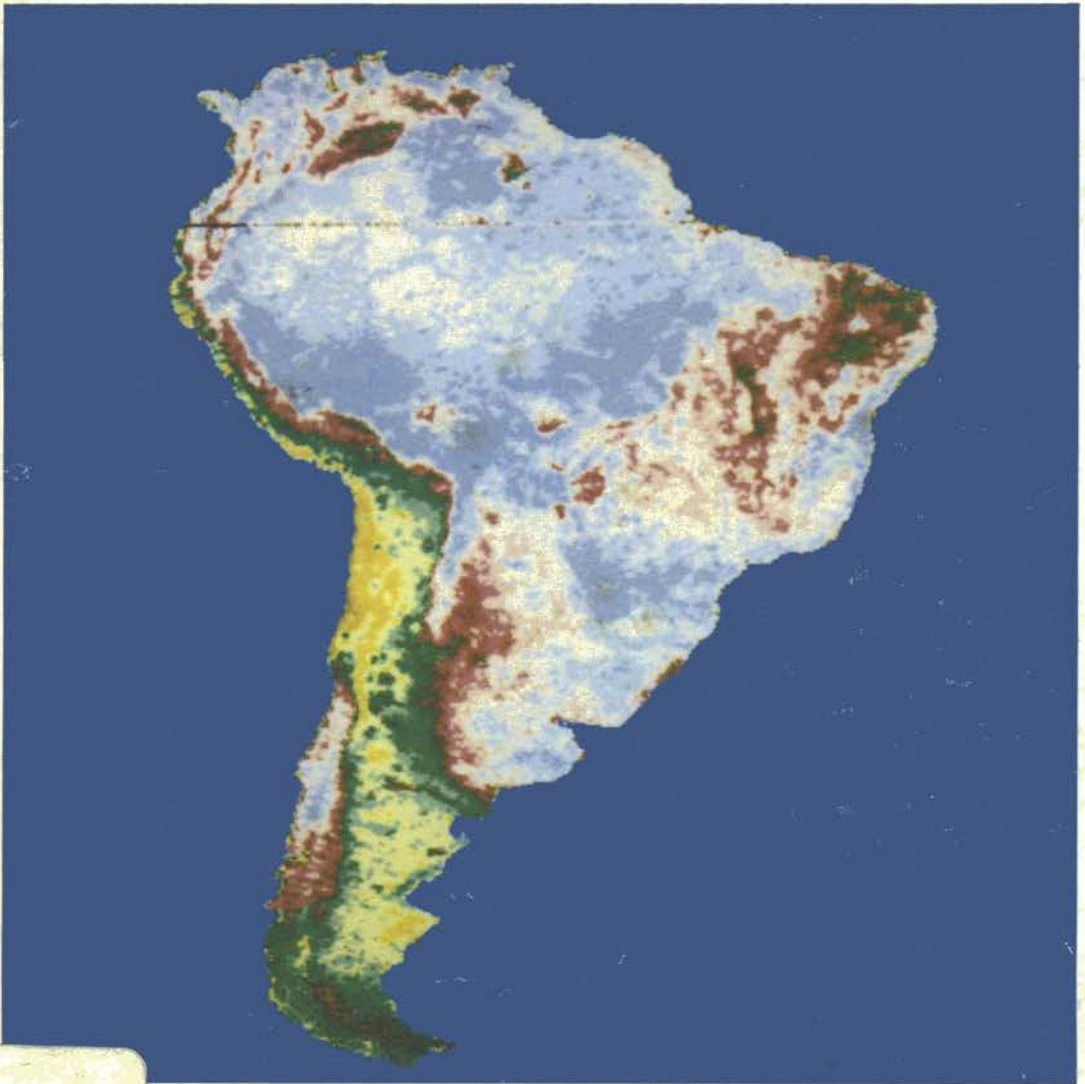
Reprinted from *International Journal of Remote Sensing*

Vol. 6 No. 8 August 1985



Analysis of the phenology of global vegetation using meteorological satellite data

C. O. JUSTICE, J. R. G. TOWNSHEND, B. N. HOLBEN and C. J. TUCKER



Global Environmental Monitoring Systems Programme



17/80
321
2-36

GEMS Programme

The Global Environment Monitoring Programme (UNEP), is a collective effort of the world community to acquire through global monitoring the data which are needed for rational management of the environment. Monitoring activities that UNEP supports fall into five major programmes: climate related monitoring, long range transport of air pollutants, health related monitoring, oceans and terrestrial renewable resources. It is under the latter programme that this present study on global vegetation monitoring is supported.

Front Cover

NOAA/AVHRR annual integrated NDVI image (1982-1983) for South America produced from the 15 km NOAA GVI product. This image is discussed in § 3 of the following paper.

Analysis of the phenology of global vegetation using meteorological satellite data

C. O. JUSTICE

Department of Civil Engineering, University of Maryland, U.S.A.

J. R. G. TOWNSHEND

Department of Geography, University of Reading, England

B. N. HOLBEN and C. J. TUCKER

Laboratory of Terrestrial Physics, NASA/GSFC, Greenbelt, Maryland, U.S.A.

(Received 14 May 1984; in final form 5 September 1984)

Abstract. Coarse spatial resolution, high temporal frequency satellite data from the NOAA/AVHRR system are presented to demonstrate their utility for monitoring vegetation seasonal dynamics. The techniques for processing and analysing the data are outlined and examples are given for selected applications at a range of scales. Normalized difference vegetation index images are presented for the entire globe and for the continents of Africa, South America and south-east Asia, with descriptions of the seasonal dynamics of major vegetation formations as portrayed by the transformed AVHRR data. Monitoring of forest clearance in Brazil, the productivity of African grasslands, Indian tropical forest and Chinese agriculture are selected for discussion. The paper concludes that coarse-resolution satellite data provide a valuable tool for vegetation mapping and monitoring at regional and global scales.

1. Introduction

1.1. Objectives

Our objective in this paper is to examine and illustrate the value of remote-sensing data for the investigation of vegetation phenology. Specifically, we are concerned with coarse resolution meteorological satellite data and the depiction of the land cover of very large areas over time. Phenology is generally accepted as including not only the timing of recurring biological events but also their causes, especially with regard to meteorological phenomena (Lieth 1974).

The study of phytophenology is important in its own right for the insight it gives into the temporal organization, evolution and functioning of ecosystems. Consequently, knowledge of the phenology of plant communities is relevant to estimating biological productivity, understanding land-atmosphere interactions and biome dynamics, modelling vegetative inputs into biogeochemical cycles, as well as for the management of vegetation resources (Lieth 1971, Taylor 1974, Lieth and Whittaker 1975, UNESCO 1979, Sarmiento and Monasterio 1983). In the context of agriculture, phenology has been used in the planning of agricultural practices, the choice of optimum species for given bioclimatic conditions, the selection of optimum seeding dates and the prediction of harvest dates (Brown 1952, Seaton 1955, Pascale

1972, Wielgolaski 1974, FAO 1978, Podolsky 1984). Observed phenological changes are a valuable tool in the identification of vegetation cover and communities, especially where remote-sensing techniques are used (Morain 1974, Vinogradov 1977, Norwine and Greegor 1983, Tucker *et al.* 1985b).

One of the outstanding merits of remote-sensing procedures in the investigation of phenology relates to the spatially comprehensive overview of vegetation that is provided. Most early investigations surveyed the phenology of relatively small areas by the use of aerial photographs (Brunnschweiler 1957, Boesch and Brunnschweiler 1960, Olson and Good 1962, Gammon and Carter 1979). Subsequently, satellite-derived data, especially from LANDSAT, have been proposed and used for multitemporal surveys of larger areas (Steiner 1969, Dethier 1974, Rouse *et al.* 1974, Ashley and Rea 1975, Honey and Tapley 1981). However, the value of this sensing system for monitoring is greatly restricted by the 18 day overpass frequency, which, for areas with consistently high cloud cover, results in insufficient images being available for phenological changes to be properly observed. We describe here how relatively coarse spatial resolution multispectral data acquired daily by meteorological satellites can be processed digitally to provide regularly available images which are by and large cloud-free for the entire globe.

This paper examines and evaluates how the resultant images for the period April 1982 to November 1983 display phenological changes at a very broad range of scales, from subcontinental to global. Relating these observed changes to ground and additional satellite-sensor-derived measurements is the subject of continuing research. This research effort forms part of the GIMMS (Global Inventory Monitoring and Modeling Studies) programme at the NASA Goddard Space Flight Center (GSFC).

1.2. *The Advanced Very High Resolution Radiometer*

On the polar orbiting satellites NOAA-6, -7 and -8, the Advanced Very High Resolution Radiometer (AVHRR) provides digital data, in the visible, near-infrared and thermal channels of the electromagnetic spectrum (Schwalb 1982, Kidwell 1984). The first spectral channel is in a part of the spectrum (0.58–0.68 μm) where chlorophyll causes considerable absorption of incoming radiation and the second channel is in a spectral region (0.725–1.1 μm) where spongy mesophyll leaf structure leads to considerable reflectance. This contrast between the two channel responses can be conveniently shown by a ratio transform, i.e. dividing one channel by the other. Several ratio transforms have been proposed for studying different land surfaces (Jordan 1969, Krieger *et al.* 1969, Tucker 1979). The normalized difference vegetation index (NDVI) is one such ratio, which has been shown to be highly correlated with vegetation parameters such as green-leaf biomass and green-leaf area and hence is of considerable value for vegetation discrimination (Curran 1980, Holben *et al.* 1980, Tucker *et al.* 1981, Hatfield 1983, Jackson *et al.* 1983):

$$\text{NDVI} = (\text{Ch2} - \text{Ch1}) / (\text{Ch2} + \text{Ch1})$$

where Ch1 represents data from the visible channel (0.58–0.68 μm) and Ch2 represents data from the near-infrared channel (0.725–1.1 μm). Moreover a ratio between bands is of considerable use in reducing variations due to surface topography (Holben and Justice 1981) and in compensating for variations in radiance as a function of Sun elevation for different parts of scenes. The latter is especially valuable when studies are made at a continental scale. However, it should

be noted that ratioing does not eliminate additive effects due to atmospheric attenuation (Holben and Justice 1981). The rationale behind the NDVI and vegetation relationship holds generally, but it should be noted that due to the complexity of ground data collection the relationship between the NDVI and green-leaf activity has been examined only for a selected number of vegetation types, principally cultivated crops.

Of the three NOAA satellites with AVHRR sensors, NOAA-7 is the prime source of data for land-cover investigations recording data at 14.30 hours local solar time. At this time the cloud cover is often higher than that found on images derived from NOAA-6 and NOAA-8 which have daylight equatorial crossings at approximately 07.30 hours local solar time. However, images from the latter usually contain large areas not illuminated by the Sun. A description of the primary spacecraft and sensor characteristics for the NOAA/AVHRR systems currently in orbit are given in table 1.

The standard NOAA/AVHRR product, collected worldwide on a daily basis since 1979, is the GAC (global area coverage) data with a 5 km × 3 km resolution element (Schwalb 1982, Gatlin *et al.* 1983). This is produced by on-board processing of the raw 1.1 km × 1.1 km LAC (large area coverage) data which for sample areas may be transmitted to Earth by special request. Since April 1982 GAC products have been used to generate a third product, called the GVI (global vegetation index) (NOAA 1983, Tarpley *et al.* 1984). This product reduces the effects of cloud cover by compositing geographically registered data sets over weekly imaging periods. Each day the NDVI is calculated and the data are resampled to a polar stereographic

Table 1. Characteristics and status of the NOAA/AVHRR systems.

TIROS-N, launched October 1978, NASA funded protoflight					
NOAA-6, launched June 1979, NOAA funded					
NOAA-7, launched June 1971, NOAA funded					
NOAA-8, launched March 1983, NOAA funded					
NOAA-9, launched December 1984, NOAA funded					
Coverage cycle	9 days				
Scan angle range	± 55.4°				
Ground coverage	2700 km				
Orbit inclination	98.8°				
Orbital height	833 km				
Orbital period	102 min				
I FOV	1.39–1.51 mrad				
Ground resolution	1.1 km (nadir); 2.4 km (max. off-angle along track); 6.9 km (max. off-angle cross track)				
Quantization	10 bit				
Equatorial crossing	<i>Des.</i>	<i>Asc.</i>			
	07.30	19.30	(NOAA-6 and NOAA-8)		
	14.30	02.30	(NOAA-7 and NOAA-9)		
Spectral channels	1	2	3	4	5
Spectral range (µm)	0.58–0.68†	0.725–1.1	3.55–3.93	10.3–11.3	11.5–12.5‡
	Status as of January 1985				
NOAA-6	Taken out of operational service 5 March 1983. Reinstated 22 June 1984.				
NOAA-7	Operational				
NOAA-8	Taken out of operational service 12 June 1984				
NOAA-9	Operational status, January 1985				

† Channel 1 range on TIROS-N: 0.55–0.90.

‡ Not on NOAA-6 or NOAA-9

projection with a 15 km resolution at the Equator which decreases to 25 km at 60°N. The sampled pixels which make up the composited image are those with the highest NDVI for each weekly imaging period. Since the daily data are spatially registered, cloud cover can be reduced by selecting for each pixel the NDVI from the day with the maximum value. Taking into account both the temporal and spatial sampling involved, each pixel selected for the weekly GVI is undersampled by a factor of at least 20. Thus, the probability of generating cloud-free imagery is high for most parts of the world. As described later in the paper, we have temporally composited these weekly images in order to reduce cloud cover further. As well as reducing clouds, this technique is effective in rejecting pixels from off-nadir positions which tend to suffer most from atmospheric scattering and subsequently have lower NDVI values (Holben and Fraser 1984).

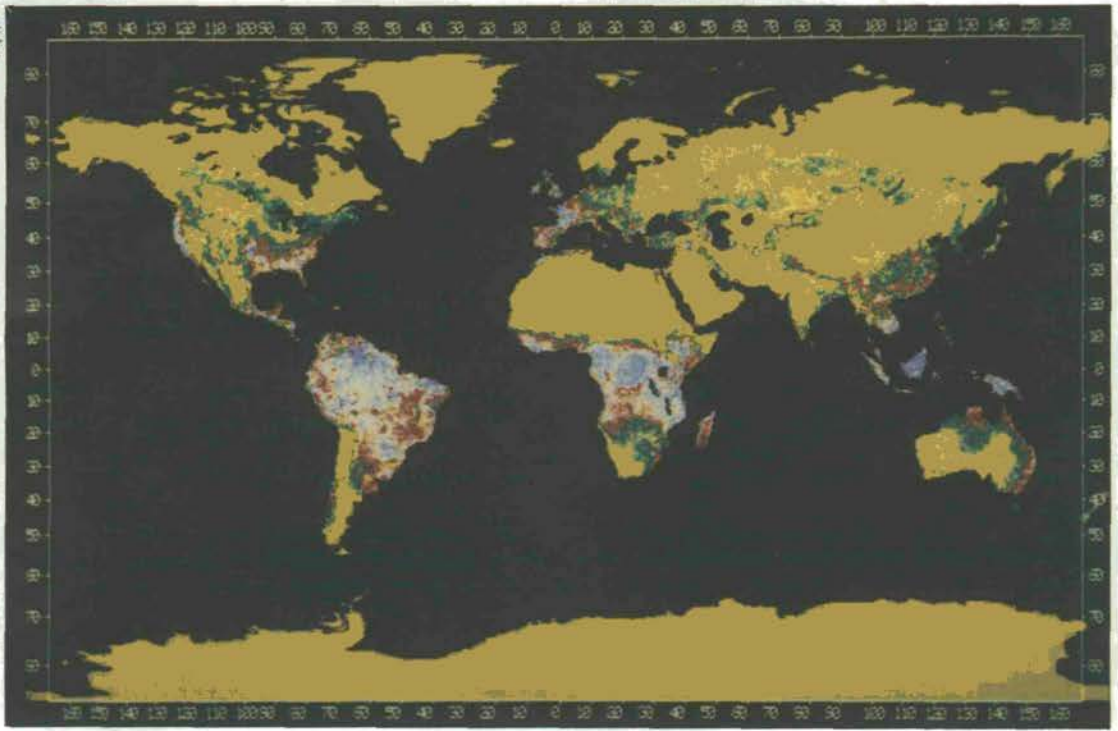
Meteorological satellite systems other than the AVHRR could in theory be used for monitoring vegetation cover, including geostationary satellites like METEOSAT (Myers 1983). However, these satellites have not had the selection of bands to allow calculation of a ratio such as the NDVI.

Several investigations of the use of AVHRR data have been concerned with single date observations (see, for example, Cicone and Metzler 1982, Ormsby 1982). Schneider *et al.* (1981) gave examples of potential applications for multitemporal AVHRR data for ice, snow and water monitoring. Norwine and Greegor (1983) demonstrated how the AVHRR NDVI could be used to monitor and stratify vegetation across a climatic gradient in Texas. LAC data were used to monitor the development of crops through the growing season in the Nile Delta (Tucker *et al.* 1984a) and to monitor grassland production in Senegal (Tucker *et al.* 1983). Tucker *et al.* (1985a) successfully used AVHRR multitemporal data as part of a multilevel sensing approach to monitor locust breeding areas. Apart from these preliminary studies, high temporal resolution data for vegetation analysis has received little consideration, yet this is undoubtedly one of the roles for which the AVHRR sensing system is best suited. In the following sections of this paper AVHRR NDVI products at different scales are evaluated for selected vegetation monitoring tasks. In the first section, global data are analysed for four different dates. In the subsequent three sections, vegetation studies from three continents South America, Africa and south-east Asia are presented both at continental and regional scales.

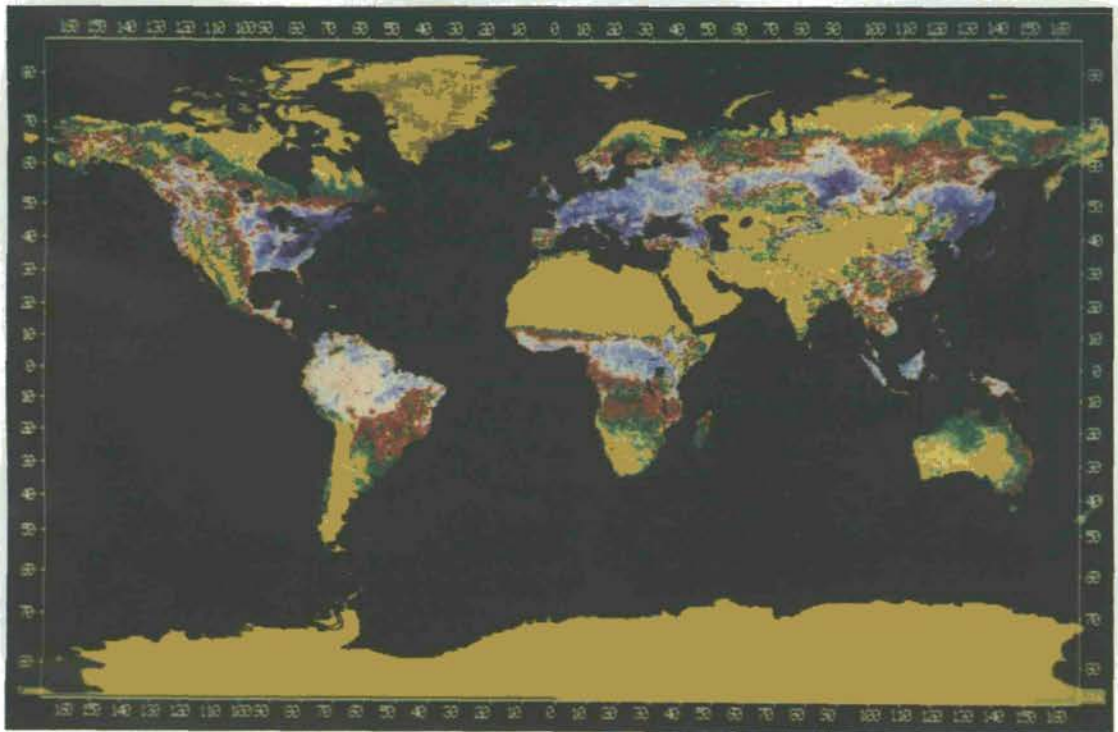
2. Global vegetation images

Accurate quantitative information on the distribution and phenology of the world's vegetation formations is extremely limited and yet is fundamental for the effective management of the Earth's resources. Such information is a basic requirement for the development of global biogeochemical and climate models and to develop an understanding of the dynamics of the major ecosystems (Bolin 1984). To date, the best estimates of the areal extent of the major vegetation formations of the Earth are compilations and syntheses of data from existing map sources (Olson and Watts 1982, Matthews 1983) or predictions of vegetation distribution based on controlling environmental parameters (Holdridge 1947, Mather and Yoshioka 1968, Box 1981). Quantifying the seasonal activity of vegetation on a global scale has received

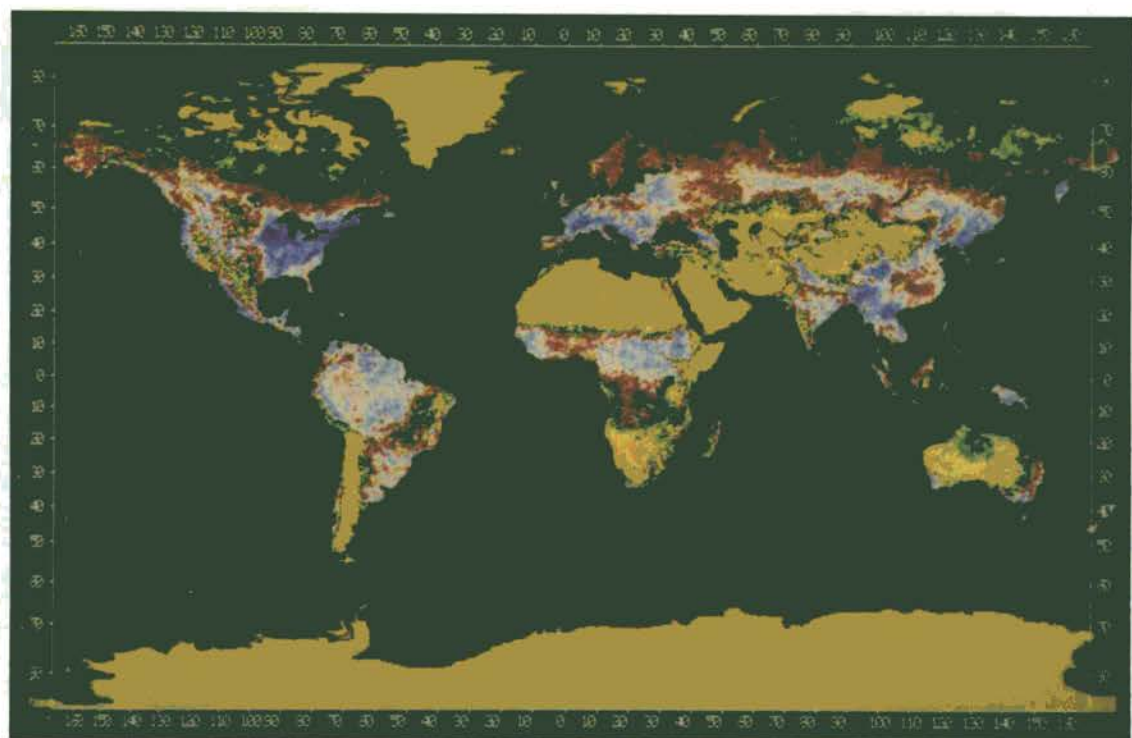
Figure 1. (a) Global NDVI composite for 12 April to 15 May 1982. (b) Global NDVI composite for 14 June to 18 July 1982.



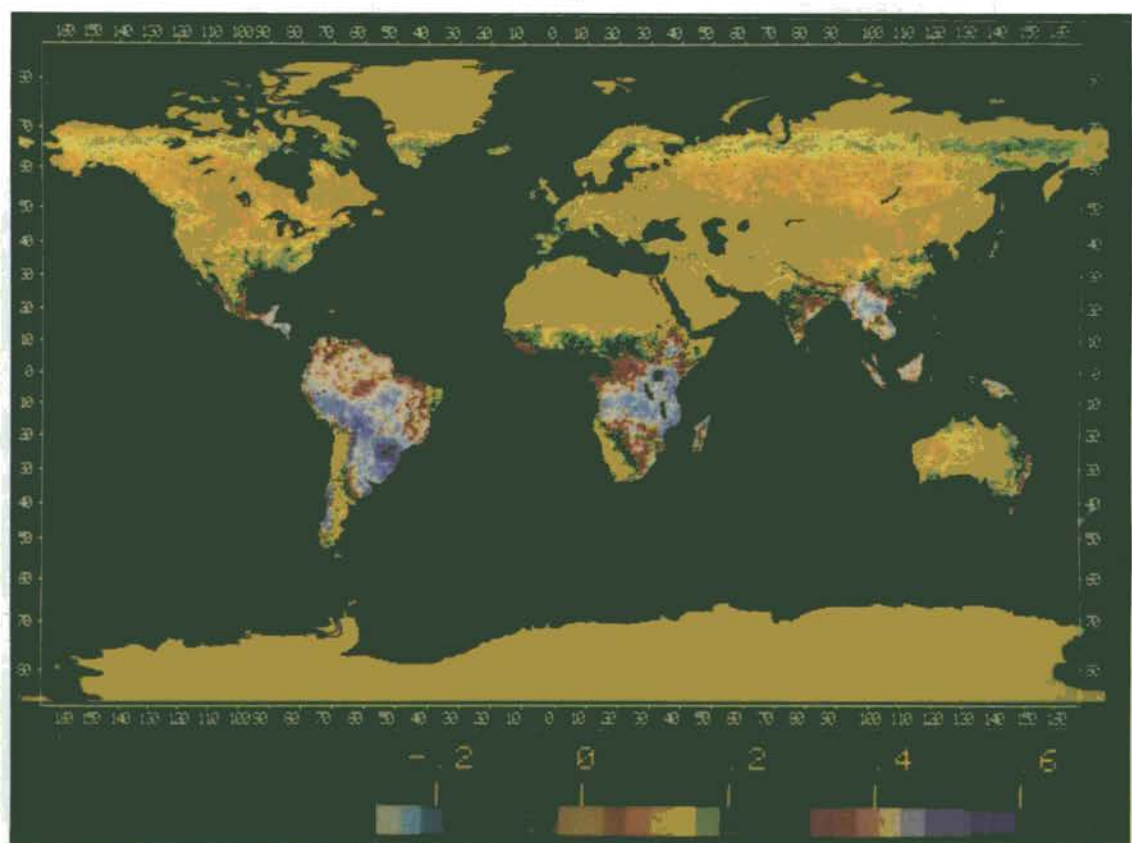
(a)



(b)



(c)



(d)

relatively little attention in the literature due to the inadequacy of existing databases (Jung and Czeplak 1968, Fung *et al.* 1983).

Figure 1 presents, so far as we are aware, the first published global overview of vegetation activity, which is represented in these images by the NDVI. Four different time periods have been selected to show the main seasonal changes. A 4-week compositing period has been chosen to reduce cloud effects worldwide. This composite was derived by selecting the highest value of the NDVI from four sequential weekly GVI products. For the purposes of display these products have been sampled by a factor of 4 and this accounts for their somewhat grainy appearance. Subsequent sections of the paper discuss and display GVI images with full resolution. The NDVI is a bounded ratio with values from -1 to $+1$. However, values for land surfaces commonly range from -0.1 to $+0.6$. To facilitate comparison, the same colour coding has been applied to each of the NDVI images represented in this paper by assigning blue, brown, green, red and purple colours to increasing NDVI values from -0.2 to $+0.6$. The colour coding and NDVI scale adopted for these images is provided in figure 1 (*d*) and is applied to all the NDVI images presented in the text.

In the first global image, covering the period from 12 April to 15 May 1982 (figure 1 (*a*)), the highest NDVI values are found near the equator, in the tropical rain forests and adjacent moist savannas. High values elsewhere are found only in the eastern U.S.A., western Europe and eastern China. Low values are found not only in the desert areas but also in India, much of Canada, the west African grasslands, the north European plain and the Soviet Union. At this time remarkably high values are found in the arid and semi-arid parts of Australia.

The next image derived for the period from 14 June to 18 July 1982 (figure 1 (*b*)) shows a dramatic change especially for mid-latitude agricultural areas in the northern hemisphere. A belt of high NDVI values represented by the mauve and purple colours is almost continuous across the global landmass. The highest values are found in the eastern U.S.A. and Canada, in western Europe and in the U.S.S.R. from Latvia almost to Lake Baykal and then again in the eastern-most parts of the U.S.S.R. north of Vladivostok. These areas correspond to the main grain-growing areas of the northern hemisphere, though the values for central and eastern U.S.S.R. are higher than the levels of agricultural activity that are indicated in existing sources of economic and agricultural geography.

North of these agricultural areas marked, though less dramatic, changes of the NDVI are found in the northern boreal forests. In Africa there has been a general northward shift of the main areas of high NDVI and a decrease in values in Angola and Mozambique. In South America the seasonal forest and tropical savannas of south-east Brazil show a decrease in the NDVI, whereas the tropical rain-forest areas of the Amazon remain constant with overall high values.

The third image is for the period 13 September to 17 October (figure 1 (*c*)). Although the northern hemisphere mid-latitude agricultural areas continue to have higher NDVI values than in the April–May image, most areas have declined significantly from the high of June–July. This arises presumably because of harvesting but also because other crops will have ripened and become senescent. High values remain, however, in the eastern half of the U.S.A., probably because of

Figure 1. (*c*) Global NDVI composite for 13 September to 17 October 1982. (*d*) Global NDVI composite for 13 December 1982 to 16 January 1983.

the importance of crops such as corn which remain green until their harvesting in September and October. In contrast, the agricultural lands of Uruguay and southern Brazil show large increases in the NDVI with the onset of the southern spring. South-east Asia shows the maximum values at this date. India has high NDVI values for most of its land area. This onset of greenness in fact occurred shortly after the June–July composite was obtained. In East Africa in Tanzania, Kenya, Zambia and Zimbabwe NDVI values are low, corresponding to the dry season which lasts until the onset of the short rains later in the year.

On the image for 13 December to 16 January (figure 1 (d)) high NDVI values are found throughout East Africa and across the continent to the Bie Plateau of Angola. In South America the highest NDVI values are found south of the rain forest in a zone stretching from Bolivia through Paraguay to southern Brazil and Uruguay which had high NDVI values in the previous image. This zone now also extends southward to the grain-growing areas of the pampas of Argentina and the agricultural areas of Chile.

This latter image also displays some of the most marked atmospheric effects and it is appropriate at this stage to discuss the limitations of this product. Across the northern part of figure 1 (d) spuriously high values of the NDVI are found. Similar effects can be detected in the southern hemisphere in Patagonia, in the June–July image. This is called the terminator effect and arises from the low winter solar illumination levels and differential transmissivity in the red and near-infrared parts of the spectrum. In the winter months irradiance is low for high latitudes because of low solar elevations. Moreover, the radiation has to pass through a considerable thickness of atmosphere. The atmosphere absorbs shorter wavelengths most and hence the difference between the red and near-infrared recorded values is increased, resulting in spuriously high NDVI values. Poleward of the region of high NDVI area, no illumination is received and hence the NDVI values drop to zero. The September–October image shows an area south of the Taimyr Peninsula, U.S.S.R., which would seem to be affected by cloud cover which has not been removed by the compositing process. Similar problems of very high frequency cloud cover also seem to be depressing the NDVI values over the islands of Indonesia on the same image and over the Amazon Basin in the December image. Current research is expected to lead to a reduction of the terminator effect by modelling, and a more effective signalling of the presence of cloud by use of a thermal channel.

Despite these limitations, these images are remarkable for the overview provided of the Earth's vegetation. It should be stressed that they understate considerably the full resolution of the GVI data and hence the detail of information which can be extracted. In the following two sections the information obtainable from the full resolution GVI products is outlined for South America and compared with GAC and LAC products.

3. South American phytophenology

3.1. Continental spectral characterization

The weekly composited GVI product provides a means by which to monitor vegetation at a continental scale for a variety of time periods. In the following example thirteen 4 weekly periods were composited to provide an annual data set for South America from 12 April 1982 to 10 April 1983. The 4 week compositing period was selected to reduce cloud contamination which is often evident within the weekly images for tropical areas. The spectral phenology of selected major biomes within

the continent was examined by producing temporal plots from known sample sites (figure 2). Fourteen vegetation types were selected to demonstrate the variability in the NDVI response over time. For each cover type three locations were selected and plotted from within the same general region to give an indication of the internal variability of the NDVI associated with the vegetation types. The individual location of the sample sites are shown on the integrated GVI image for the 1 year period (figure 2 (a)). The temporal plots corresponding to each location are presented in figure 2 (b). Each data point on the plot represents the average value for a matrix of 3×3 pixels around the selected pixel location corresponding to approximately 2000 km^2 on the ground. The locations and the following description of the vegetation formations are given by reference to Scholten's description of the vegetation of South America from the memoir to the *FAO/UNESCO Soil Map of the World* (FAO/UNESCO 1971), the *1:5 000 000 UNESCO Map of the Vegetation of South America* (UNESCO 1980 a) and the authors' field experience.

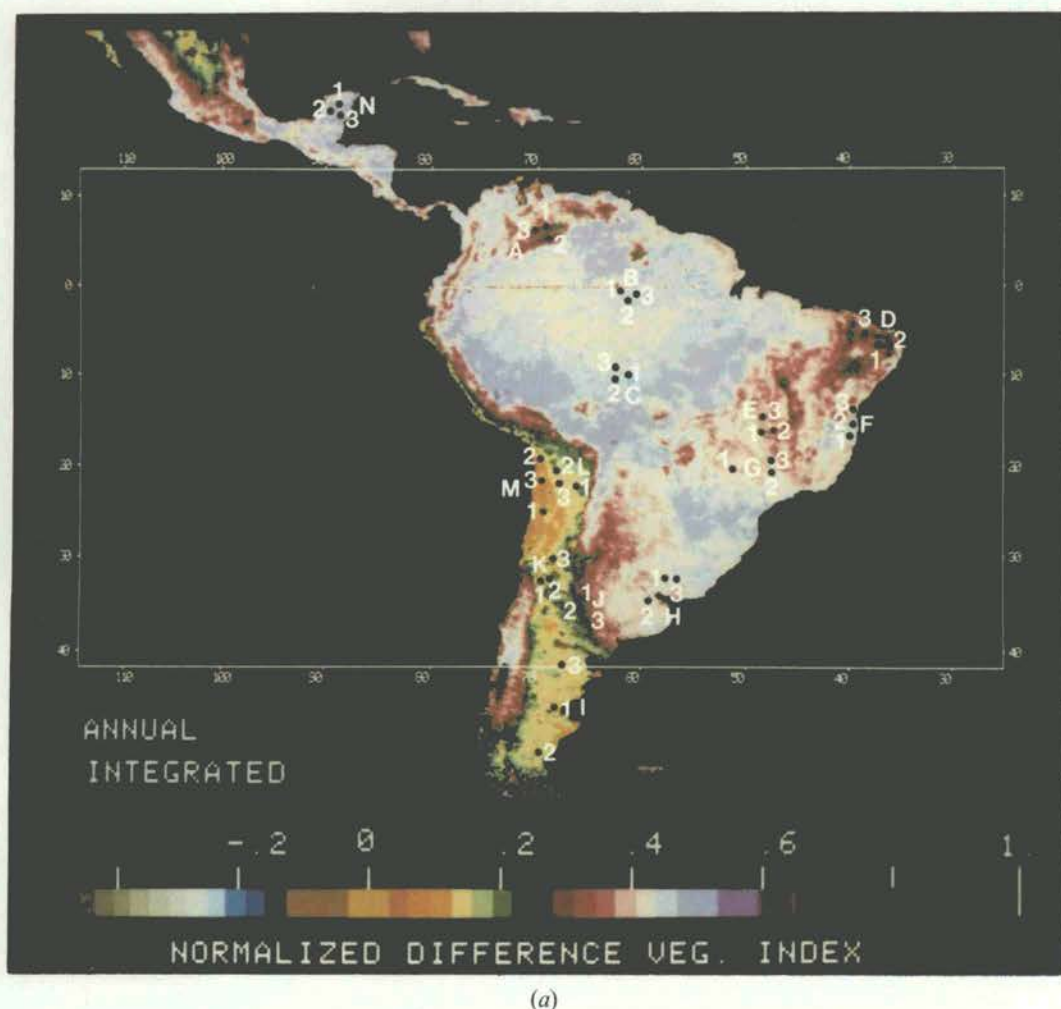
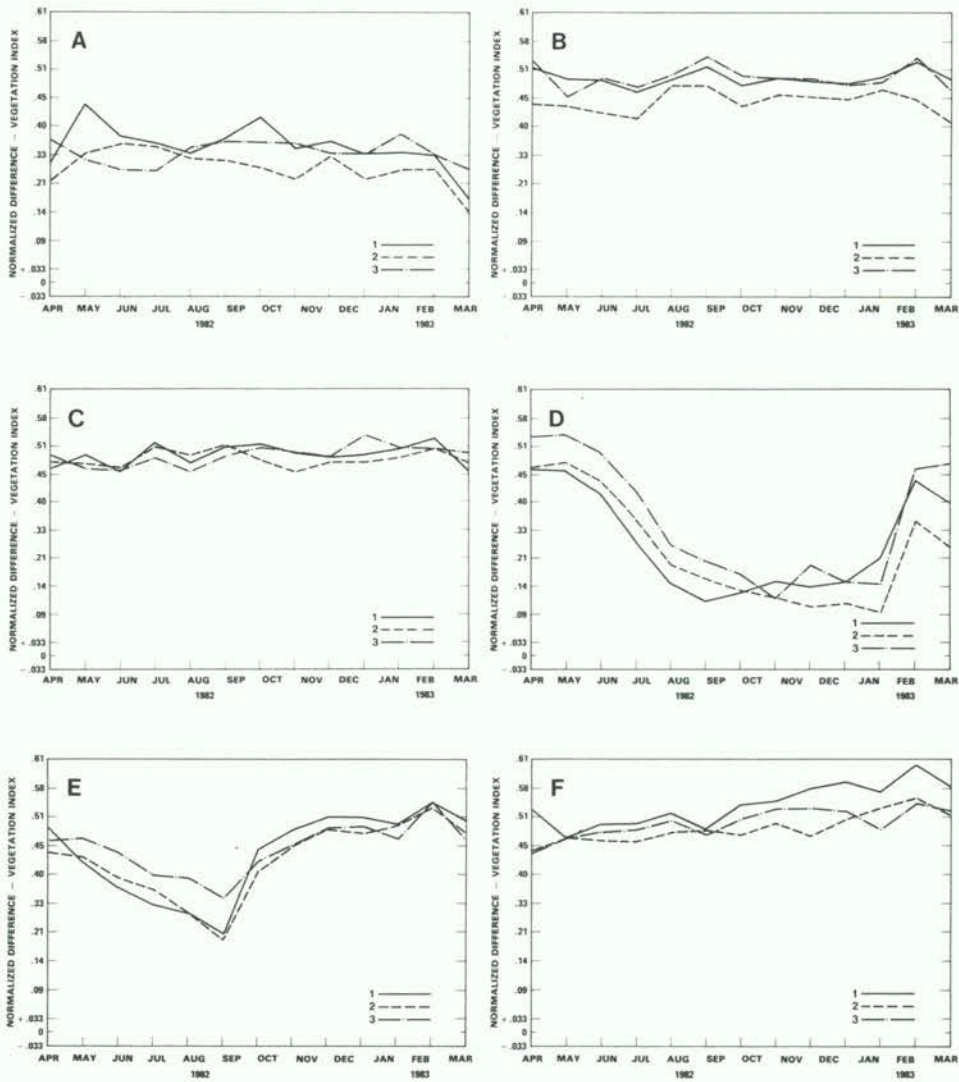


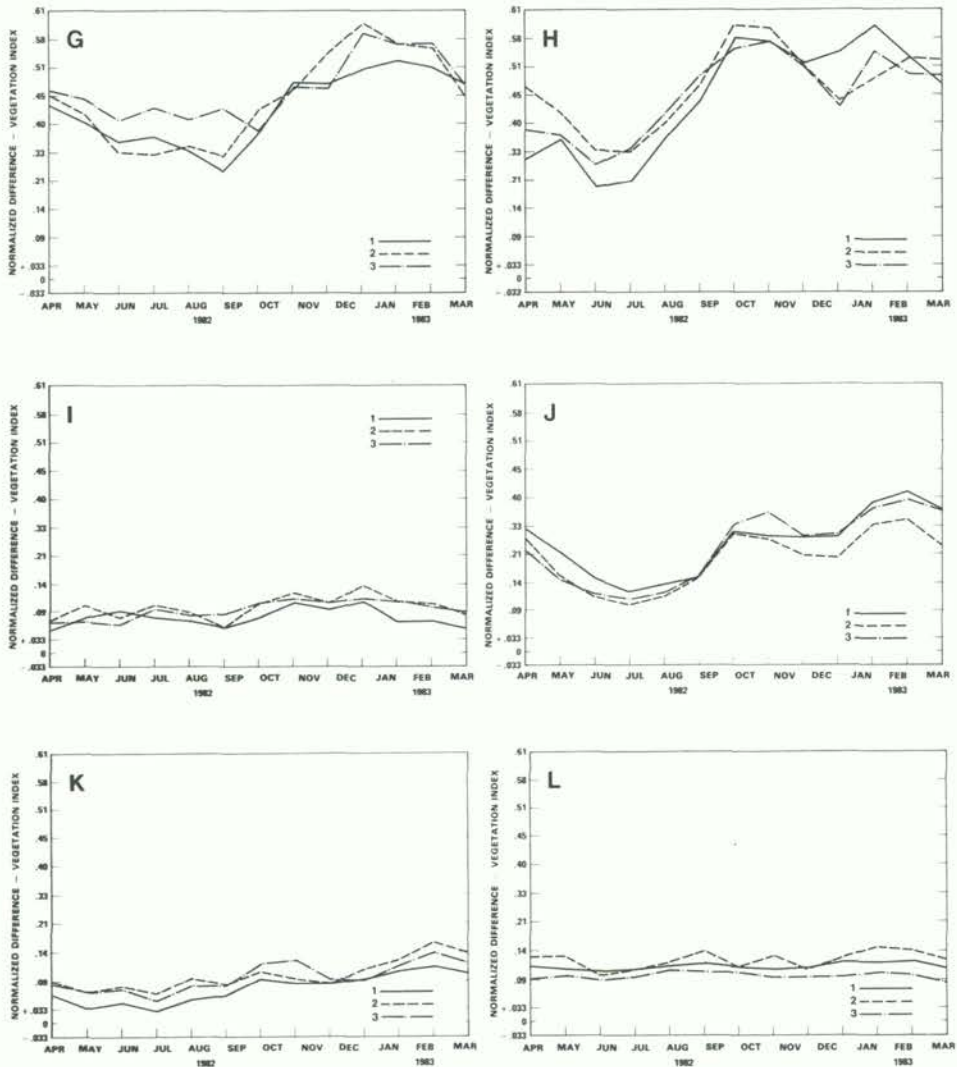
Figure 2. (a) An annual integrated image (1982-1983) showing the location of the sites used in producing the spectral-temporal plots of (b). (b) Spectral-temporal plots of selected South American cover types (1982-1983).

Comparison of the AVHRR temporal NDVI plots show a wide range of patterns associated with the different cover types (figure 2 (b)). Plot M represents the Pacific coastal desert which is extremely arid and barren and shows low NDVI values throughout the year. Plots I, L and K represent three different forms of steppe and display similar patterns with a generally low NDVI throughout the year. A marked increase in the NDVI during the southern hemisphere summer can be seen in the plots for the wooded steppe of west Argentina (plot K). Plot D represents the scrub and thorny woodland of the Caatinga of north-east Brazil and shows considerable variation in the NDVI throughout the year. The high values of this unimodal distribution are associated with the humid season between January and July. Plot A represents the Llanos of the Orinoco which consists of several types of savanna. The

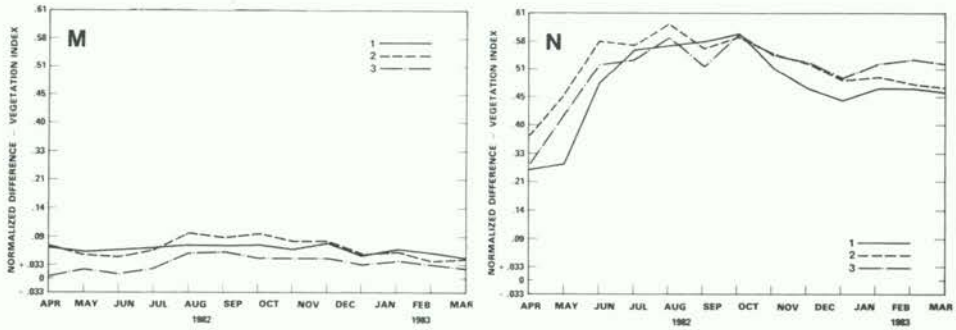


(b)

NDVI values are higher throughout the year than for the steppe plots. Plots G and J for the dry pampas and the agricultural area of south-east Brazil exhibit similar patterns in the NDVI throughout the monitoring period, with low values between the winter months of May and October which gradually increase to maximum values from January to March. The values for the agricultural humid pampas of Argentina (plot H) show a similar range of values to plot G but with a peak NDVI period between September and November. The wooded savanna of the Mato Grosso (plot E) show generally high values throughout the year with lower values occurring at the end of the winter between July and September. Plots B, C, F and N represent different types of tropical forest showing high NDVI values throughout the year for the rain forest and seasonal rain forests of the Amazon.



(b)



- A** – Savanna, Eastern Llanos, Orinoco
- B** – Tropical Rain Forest, Amazonas
- C** – Tropical Seasonal forest, Amazonas/Rondonia
- D** – Scrubland and Thorny Woodland (Caatinga), N.E. Brazil
- E** – Wooded Savanna (Cerrado), Mato Grosso
- F** – Tropical Coastal Rain Forest, Bahia, Brazil
- G** – Mixed Agriculture and Forest, San Paolo, Brazil
- H** – Agriculture, Humid Pampas, Argentina
- I** – Steppe, Patagonia, Argentina
- J** – Agriculture (Wheat), Dry Pampas, Argentina
- K** – Wooded Steppe, W. Argentina
- L** – Arid Steppe, Altiplano, Bolivia
- M** – Pacific Coastal Desert, Atacama, Chile
- N** – Tropical Forest, Yucatan, Mexico

(b)

3.2. Comparison of AVHRR data product resolutions: Rondonia, Brazil

The maximum spatial resolution of AVHRR data is 1.1 km at the nadir, based on a IFOV of 1.4 mrad and a mean altitude of 850 km. These LAC data are available only upon special scheduling of the recorders on board or through direct transmission from the satellite. As outlined above, GAC and the GVI product have significantly coarser resolutions of 4 and 15 km, respectively. As a comparison of the potential information available from these three data types we have examined the Amazon Basin, focusing on deforestation within the state of Rondonia in southern Brazil.

Rondonia is currently undergoing rapid forest conversion which is occurring through government-planned colonization projects designed to provide inexpensive land to unemployed agriculturists in a systematic fashion. Farm lots, usually 100 ha each (500 × 2000 m) are sold to immigrants to use for crops or pasture. Each lot has 500 m of road frontage. Clearing on a lot begins nearest the access road, then gradually moves away as the farmer clears more land to maintain or increase agricultural production on soil not yet depleted of nutrients. A typical colonization has a sprawling town near its centre with parallel access roads dissecting the colonization. Extensive areas of agriculture and pasture occur adjacent to the access roads with relatively narrow strips of primary forest between. Surrounding the colonization projects is undisturbed tropical forest occupying an area of approximately 240 000 km² in Rondonia. The uniformity of the cover type is broken only by a few meandering tributaries of the Amazon river. To the south of the rain forest are the woodlands and savannas of the Mato Grosso. Major colonization projects are centred at 11°S and 61°W and extend intermittently for nearly 300 km along highway

BR-364, the major access route into the region. In some places the colonization areas are up to 80 km wide (Tucker *et al.* 1984 b). Access roads are approximately 4 km apart and fields and pastures are usually less than 2000 m on a side.

Full resolution GVI data were mapped and composited for the 4 week period from 5 July to 7 August 1982 (figure 3). As discussed previously, these data indicate contrasts in the green-leaf biomass levels between regional cover types, which appear to be closely associated with boundaries of major biomes. With this particular density slice parts of the Amazon river and its major tributaries are represented by intermittent lines of low NDVI values caused by mixed pixels of water and forest. Variations within the tropical forest are detectable at this resolution, but the colonization areas in Rondonia are undetectable. For ease of comparison the area covered by the full resolution GAC image (figure 4) is delimited by a white rectangle.

In contrast to the GVI product, a full resolution single date GAC image of a single orbit over Rondonia for 9 July 1982 is presented in figure 4. With a product at this scale, substantial variations of the NDVI within the rain-forest biome are readily detectable. The clearance areas described above appear as linear features with decreased NDVI values following the north-west-south-east orientation of BR-364. The area covered by the full resolution LAC image (figure 5) is indicated by a white rectangle.

LAC data of Rondonia were also processed for the same date to derive an NDVI image (figure 5). At the nominal 1.1 km resolution, the linear features of the access roads crossing highway BR-364 are now detectable. Many of the rivers, towns and agricultural areas are readily apparent. However, individual fields cannot be distinguished because they are of subpixel size. The detectability of the deforested areas on the LAC data make this product suitable for delineation and areal estimation of such features (Tucker *et al.* 1984 b).

The above comparison demonstrates the AVHRR data are available at a variety of scales suitable for a wide range of interpretation tasks. Although these GAC and LAC examples have been given for single-date imagery, the same frequency of multitemporal coverage is potentially available for all the scales. In addition, although the NDVI images have been presented for this example, individual AVHRR spectral bands are currently available at GAC and LAC scales.

One of the most important roles for the AVHRR data is as part of a multistage sampling approach to vegetation analysis. Clearly, for many studies the resolution of the AVHRR system will be too coarse and higher resolution satellite data will be required. To demonstrate this point the NDVI transform for a LANDSAT MSS image for May 1981 of the Rondonia site is presented in figure 6 for comparison with a black-and-white contrast enhanced LAC image of the 9 July data previously shown in figure 5. The fine detail of the clearance and rivers which are indistinguishable on the LAC image (figure 6 (a)) can be seen on the MSS data (figure 6 (b)). A comparison of the features apparent in the two LAC images in figures 5 and 6 shows that a generally applied colour-coding scheme can be unsuitable for portraying specific features represented by a narrow dynamic range of NDVI values.

4. African phytophenology

4.1. Continental spectral characterization

As part of a joint study on the status of African vegetation with the Food Security Group at the UN/FAO, the GIMMS group have developed a special African AVHRR product. This product is derived every 10 days from the daily GAC

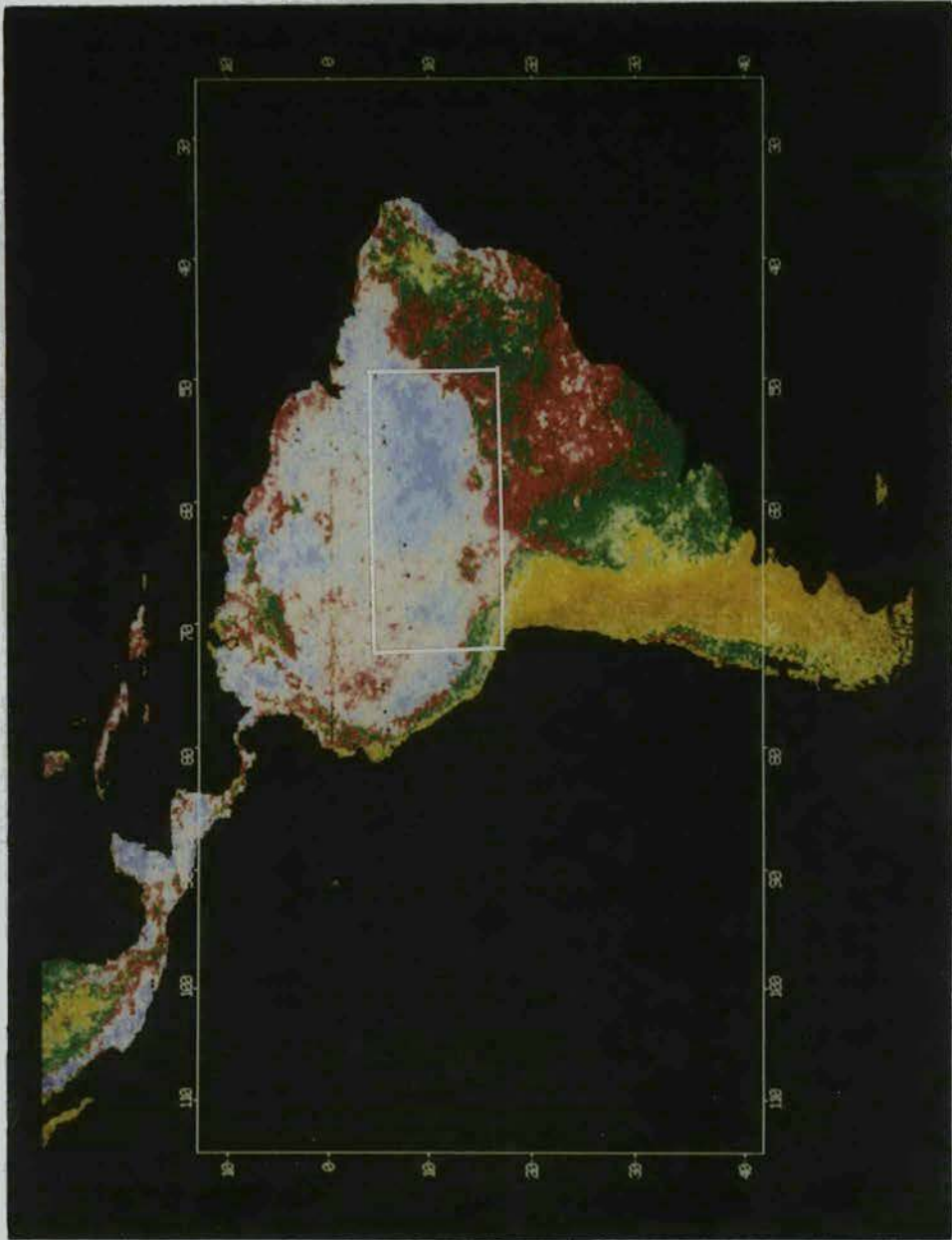


Figure 3. Full resolution GVI composite of South America outlining Rondonia, Brazil (5 July to 7 August 1982).

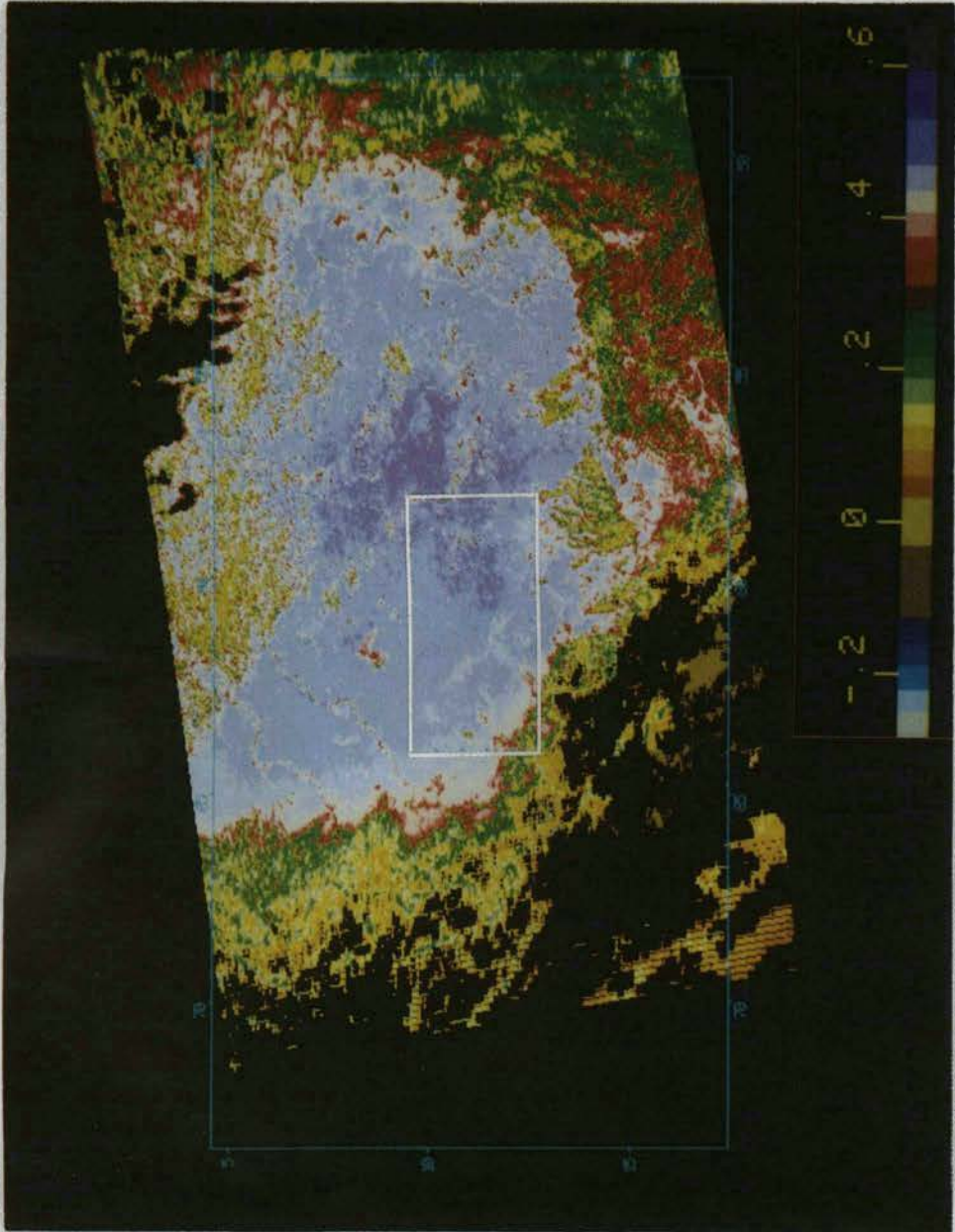


Figure 4. Full resolution GAC image for 9 July 1982 outlining Rondonia, Brazil.

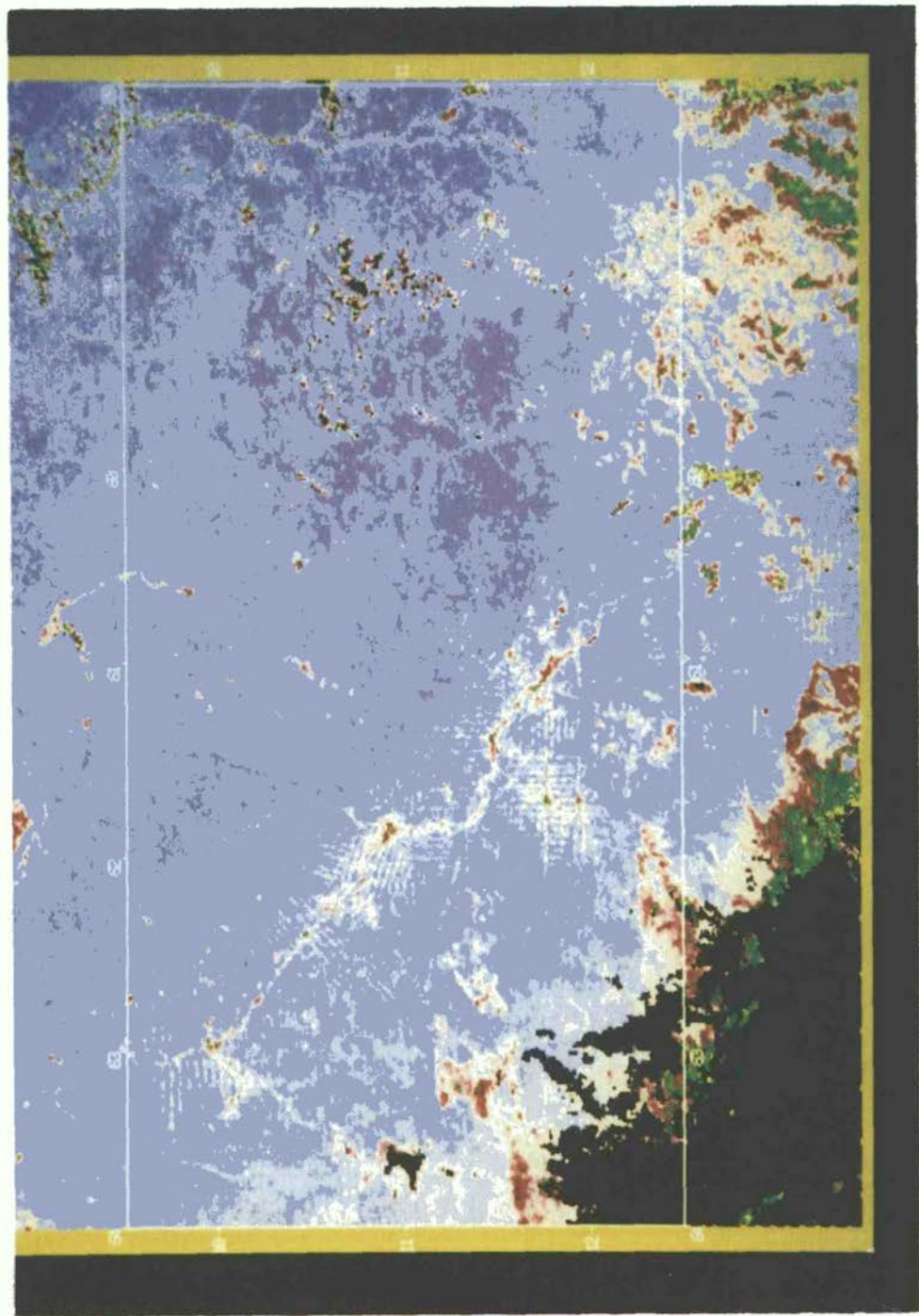
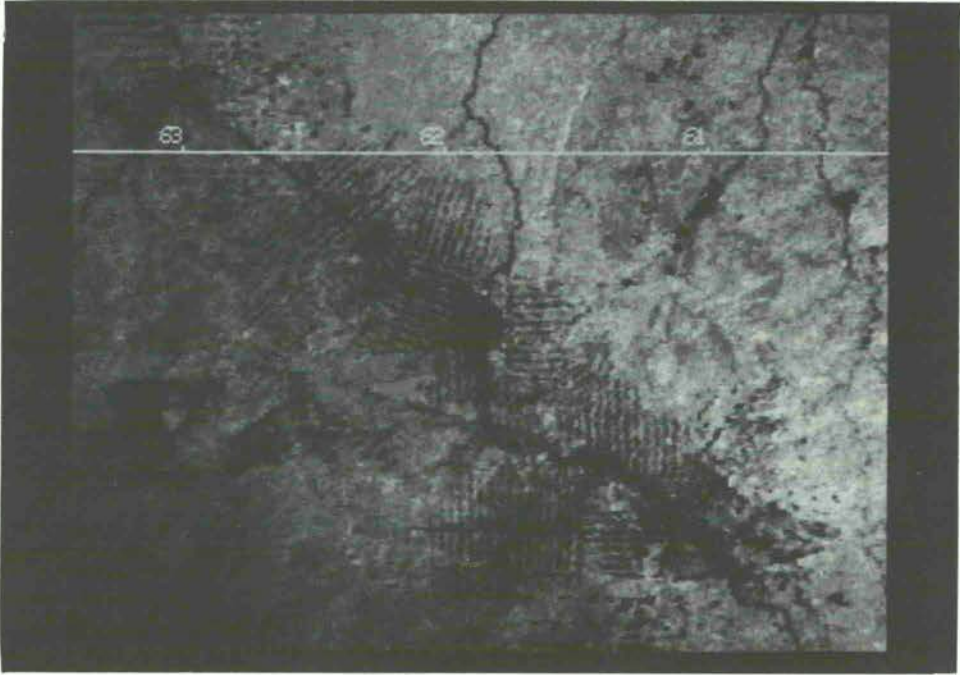


Figure 5. Full resolution LAC image for 9 July 1982 of Rondonia, Brazil.



(a)



(b)

Figure 6. Comparison of black and white contrast enhanced AVHRR LAC (a) and LANDSAT MSS, (b) data of Ji Parana, Rondonia, Brazil.

data, which is resampled to provide an 8 km nadir resolution compared with the GVI's resolution of 15 km. Ten-day composites of this African product are currently used by the UN/FAO as an integral part of their African agricultural early warning system. In the following example, four 1 month composites from May to November 1983 are used to describe the regional dynamics of the major African vegetation formations (figure 7 (a-d)). Discussion of the vegetation formations is based in part on our own field observations, but has also relied heavily on published works especially of White (1983) and information on vegetation conditions during this period were provided by the UN/FAO Food Outlook Reports and from the Agrhymet Centre in Niger.

The major desert areas of Africa, the Sahara and the Namib, have low vegetation indices for all four monthly periods. The transitional semidesert zones of the Sahel and the Kalahari show considerable fluctuation in the amount and presence of green vegetation. A comparison between the May and September images for northern Nigeria and southern Niger shows a marked northerly increase in green vegetation. The May image shows the minimum amount of green vegetation prior to the growing season across the Sahel. The annual grasses common throughout the Sahelian zone greened-up (with the start of the rains) during June and July reaching a peak in growth towards the beginning of September, portrayed by higher NDVI values for the September composite. The grasses then senesced to give the low NDVI found in the November image. AVHRR studies in Senegal and Niger for 1983 showed particularly low NDVI values in the northern Sahel associated with the below-average rains reported for that year by the Agrhymet Centre in Niger. A more detailed discussion of this 'green-wave' effect in the Sahelian zone of Senegal is presented in the following section. South of the Sahel lies the Sudanian zone where a moister climate permits extensive agriculture and where the remaining natural vegetation consists of various types of woodland and wooded grassland. The average annual rainfall distribution in West Africa is unimodal and occurs between May and October. The peak period of vegetation activity is shown in the September image followed by a marked decrease in November. The November image shows an area of low NDVI in northern Ghana which has been identified as an area of drought caused by an early end to the rainy season in 1983.

The tropical rain-forest areas of Africa occurring within the Guineo-Congolian region defined by White (1983) have high vegetation indices throughout the year. These forests are evergreen or semi-evergreen with an evergreen understory. The forests of the relatively dry periphery to the north and south are more deciduous and exhibit a well-defined dry season. The belt of rain forest from Guinea, the Ivory Coast and Ghana to Nigeria, Cameroon and Zaire is broken by the Dahomey Interval, which consists of secondary grasslands and wooded grasslands which are apparent on the May and November images.

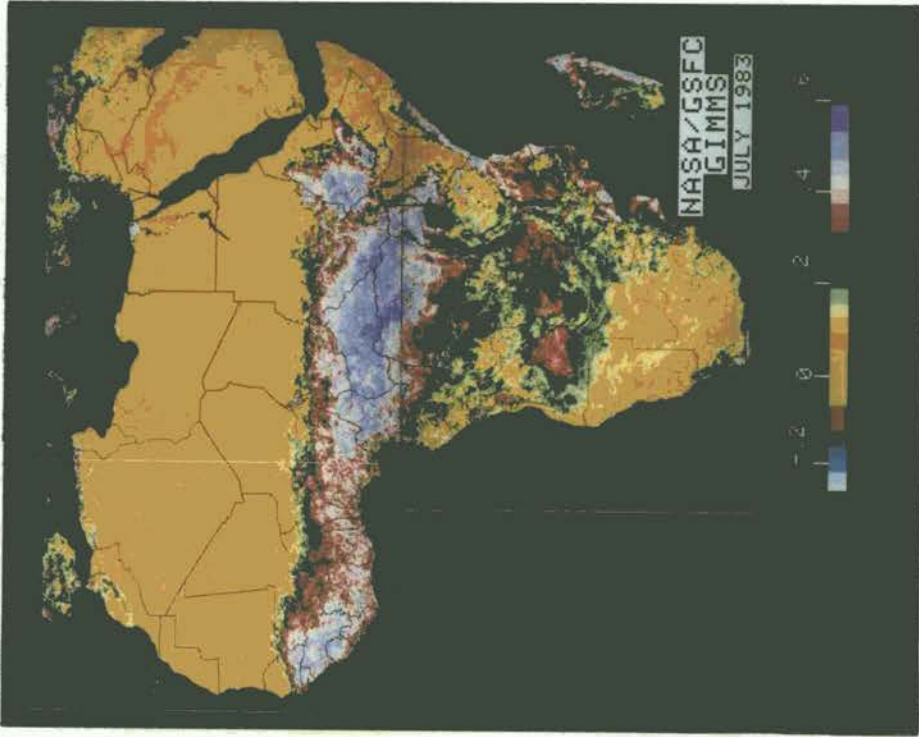
In East Africa the distribution and seasonal dynamics of the vegetation is somewhat different due in part to a bimodal rainfall distribution and a considerable range in relief (Brown and Cocheme 1973). The physiographic region of the Ethiopian highlands stands out on the AVHRR imagery as an area of consistently high NDVI and corresponds to the response from undifferentiated montane forest, evergreen and semi-evergreen bush and thicket and montane woodland. To the west of this region in southern Sudan lies an area of edaphic grassland which is clearly differentiated on the AVHRR imagery, exhibiting a low NDVI in May, increasing to similar values as the forest areas in September and decreasing in November. To the

east of the Ethiopian highlands lies the northern extension of the Somali–Masai bushland and thicket which shows an increased vegetation index with the early rains in May and a slight increase in November with the later rains. The Somali–Masai bushland and thicket extends south to Tanzania and consists predominantly of *Acacia* and *Commiphora* bush in various degrees of degradation. A field visit to the Garissa region of eastern Kenya in August 1983 revealed that the early rains had failed which is manifested by low NDVI values throughout this region in the May imagery. Field reports indicated that although there was abundant precipitation in the Kenyan highlands, the late rains were negligible (M. Gwynne 1983, personal communication). This is in accord with low NDVI values for the November image throughout this region. To the extreme east of the Ethiopian highlands in north-east Somalia and Mauretania the semidesert grassland has a consistently low NDVI throughout the four monitoring periods.

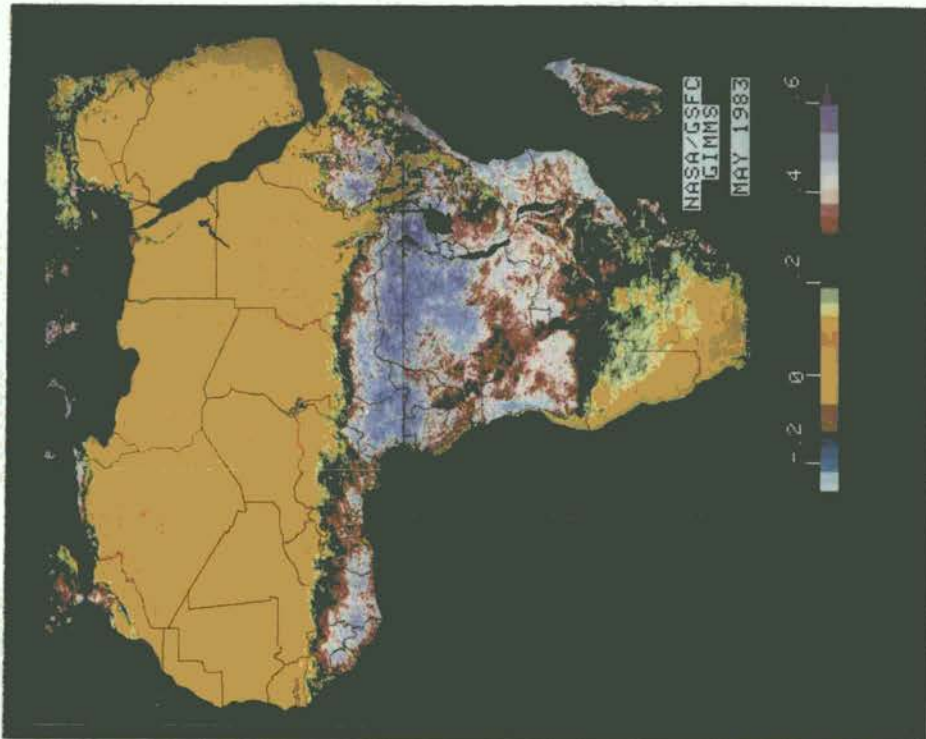
To the south of the rain forest and the forest transition zone occurs the Zambezi zone which extends from Angola in the west to Zimbabwe and Tanzania in the east (White 1983). This area is the southern equivalent to the Sudanian zone, but has a single rainy season from November to April, a cool season from May to August and a hot season from September to November. The vegetation is diverse; White (1983) defines 21 major mapping units for this zone including forest, woodland, bushland and thicket, wooded grassland and grassland types. The AVHRR data show medium to high NDVI values for May decreasing to September and increasing in the northern parts in November, corresponding to the onset of the rainy season. One of several marked features within this region is an extensive area of edaphic grassland around Mongu near the Zambian–Angola border, in the upper reaches of the Zambezi river. This area has lower NDVI values than its surrounding areas for all four time periods. Generally, low NDVI values in southern Africa in May, and the successive images, are associated with drought conditions. Unusually dry weather reported for April resulted in failure of the corn crop and shortage of irrigation water.

Several additional features of interest appear on these images. Seasonal variations in the vegetation of the Mediterranean coast of Africa from Morocco through to Tunisia can be detected. The Nile flood plain and Delta show seasonal variations with a peak period of green-leaf production in August (Tucker *et al.* 1984 a). The interior swamp lands of Lake Chad and the Sud can be clearly seen on the May image. The Niger Delta and the Okavango Swamp are depicted on the November image contrasting with surrounding areas of low NDVI values. The tropical rain forest of the Malagasy Republic stand out clearly on all four images.

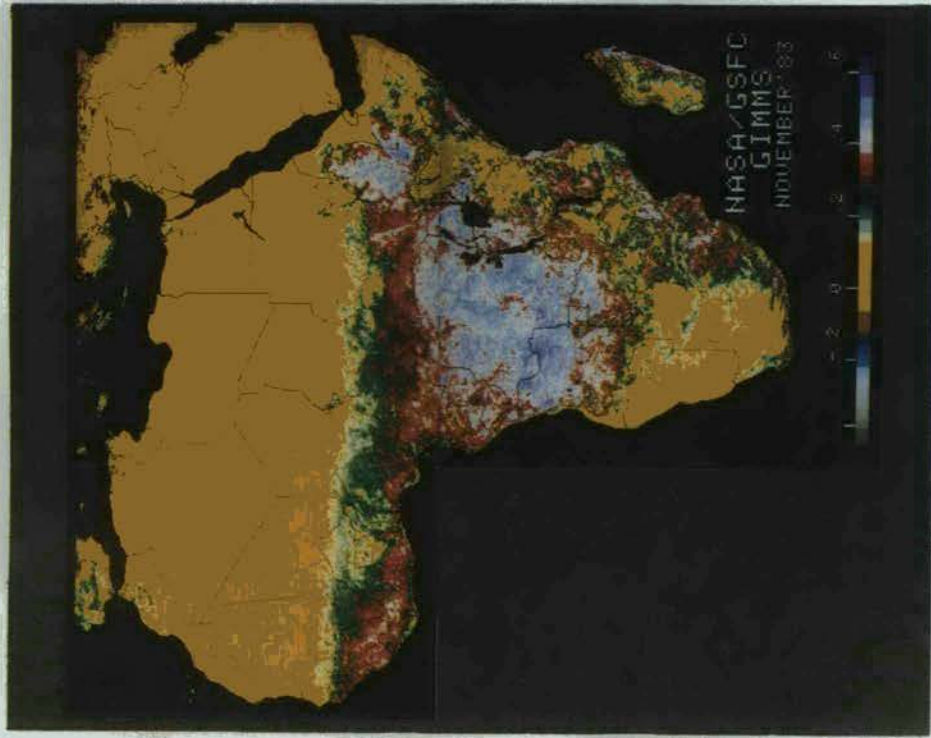
The above cursory description of some seasonal variations in the vegetation of Africa shows the unique capability of these satellite data for monitoring vegetation conditions. Once a continuous archive is established for a number of years for the different continents and our understanding of the behaviour of the NDVI for different vegetation types has developed, it will be possible to make interannual comparisons of the status of the vegetation for the different regions. As a supplement to existing drought early-warning schemes, the AVHRR data can make a valuable contribution because of its spatially comprehensive and timely coverage. In addition, research is being undertaken by the GIMMS group to use the multitemporal characteristics of the vegetation response to provide a semi-automatic classification of vegetation on a continental scale (Townshend and Tucker 1984, Tucker *et al.* 1985 b).



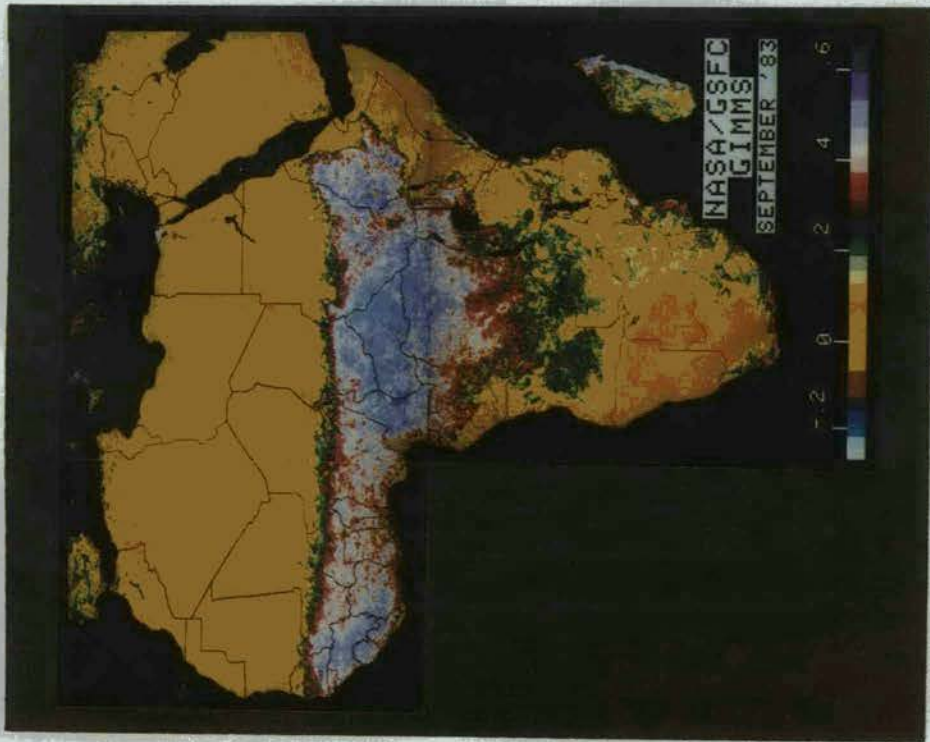
(a)



(b)



(c)



(d)

Figure 7. Four monthly composites of the African 8 km GAC product from 1983.

4.2. Monitoring the Sahelian grasslands of West Africa

Remote sensing has considerable potential as a tool for monitoring rangeland conditions (see, for example, Rouse *et al.* 1974, Honey and Tapley 1981, Vinogradov 1981, Carneggie *et al.* 1983, Grouzis and Methy 1983, Tucker *et al.* 1983) particularly if it can provide a synoptic view of grassland conditions in a timely fashion. Within the Sahel, the transient nature of the precipitation and the associated rapid vegetation response means that high-frequency monitoring is required during the 3 month growing period and over very large areas. Such coverage has been impractical to date using the LANDSAT observation system, in part due to the absence of a ground receiving station for the Sahelian zone but largely due to the LANDSAT 18 day orbit being inadequate to provide cloud-free imagery with the required frequency during the critical growing period. A survey of the LANDSAT data for the Sahel region of Senegal showed that during the rainy season (when most vegetation growth occurs), the cloud cover of the best rainy season imagery available averaged only 50 per cent (figure 8).

The multitemporal coverage of the AVHRR system and the compositing technique described previously makes high-frequency vegetation monitoring of such large areas as West Africa feasible. In West Africa mean rainfall declines northward towards the Sahara and in the absence of significant relief, the isohyets are roughly parallel to lines of latitude. Within this area lies the Sahel, the semidesert wooded grasslands bordered by semidesert grassland and shrubland to the north and the Sudanian woodland zone to the south. The Sahel is characterized climatically by a high mean annual temperature of 26–30°C and a unimodal rainfall distribution with the rainy season lasting 2–3 months between June and September (Cocheme and Franquin 1975). The rains are unreliable both in timing and spatial distribution, the location of the 100 mm isohyet was reported to vary by as much as 250 km during the 1969–1973 drought (UNESCO 1980 b). The Sahel zone is generally considered to consist of three subregions defined by their mean annual rainfall; 100–200/250 mm Sahelo-Saharan; 200/250–400 mm Sahel; 400–600 mm Sahelo-Sudanien. The vegetation of the zone reflects in part this precipitation gradient with semidesert grassland

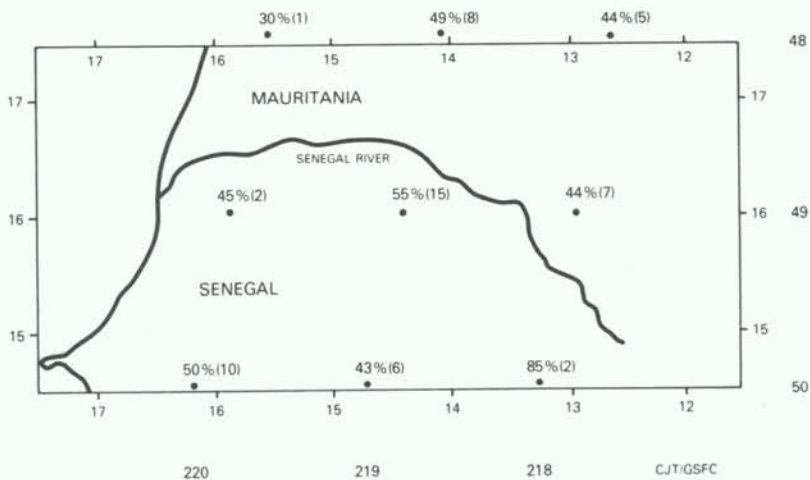


Figure 8. LANDSAT MSS average cloud cover percentages for the West African Sahel from 15 July to 15 October. The number of images since 1972 appear in parentheses.

in the north merging to (*Acacia*) wooded grassland in the south (Menaut 1983, White 1983). To quantify the phenology of the vegetation across this gradient, the NDVI values for three north-south sample transects are plotted against time for 10°W, 10°E, 30°E (figure 9). The most striking feature of these three sets of plots is the similar appearance of the curves. This similarity is marked for the most northerly sample locations representing the response from the Saharan zone. However, the increase in the peak of the NDVI curve and the increase in the duration of active green vegetation with a decrease in latitude is also common to all three transects. It is worth noting that at 14°N there is a decrease in the NDVI peak and duration from 10°W to 30°E associated with a more southerly extension of the arid conditions. The three plots demonstrate the vegetation response to the north-south precipitation gradient. This can be seen most clearly by comparing the longer duration of the growing season in the Guinean zone at 10°N with that of the Saharan zone at 20°N.

The utility of the AVHRR data for rangeland monitoring has been demonstrated by a pilot study undertaken in conjunction with FAO/UNEP to estimate total dry matter production (TDMP). The productivity of the grasslands is dependent on several factors including the dominant species, soil hydrology, grazing history and the timing, frequency and amount of useful rainfall. Failure of the rains over consecutive years can lead to severe problems of drought for the nomad population as was the case between 1968 and 1973 when over two-thirds of the cattle population was lost (UNESCO 1980 b). Information on the condition and productivity of the grasslands through the growing season and from year to year exists only for a very small number of experimental stations. Similarly, rainfall data are sparse throughout the Sahel and where available can only be representative of conditions for a very localized area.

A study in 1981 in the Ferlo region of Senegal undertook a temporal integration of the rainy season NDVI data to estimate the TDMP (Tucker *et al.* 1983). The following data are presented from this study. AVHRR LAC data were obtained from 17 August until 8 October 1981 and were integrated over the monitoring period (figure 10). A ground sampling scheme was designed and a programme of hand-held radiometer measurements and sample clipping was undertaken at the end of the growing season. The samples were weighed immediately after clipping and subsequent dry-weight measurements were made. The relationship between the end of season total above ground dry weight and the AVHRR-integrated values was established and ground-based measurements were used to calibrate the AVHRR data and to produce a preliminary areal extrapolation of estimated biomass for the Ferlo region (figure 11). The preliminary results from this study are encouraging in that they indicate that AVHRR data may be able to provide useful information to support ground-based estimates of TDMP for semi-arid grassland. This study was continued in 1982 and 1983 with encouraging results permitting analysis of the interannual variability of this region (Tucker *et al.* 1984 c). For the 1983 and 1984 growing seasons similar test sites have been established in Niger, Mali, Ethiopia, Kenya and Botswana with the aid of the International Livestock Center for Africa (ILCA), UNEP and FAO to further examine relationships between NDVI and green biomass over a wider range of grassland and savanna conditions in Africa.

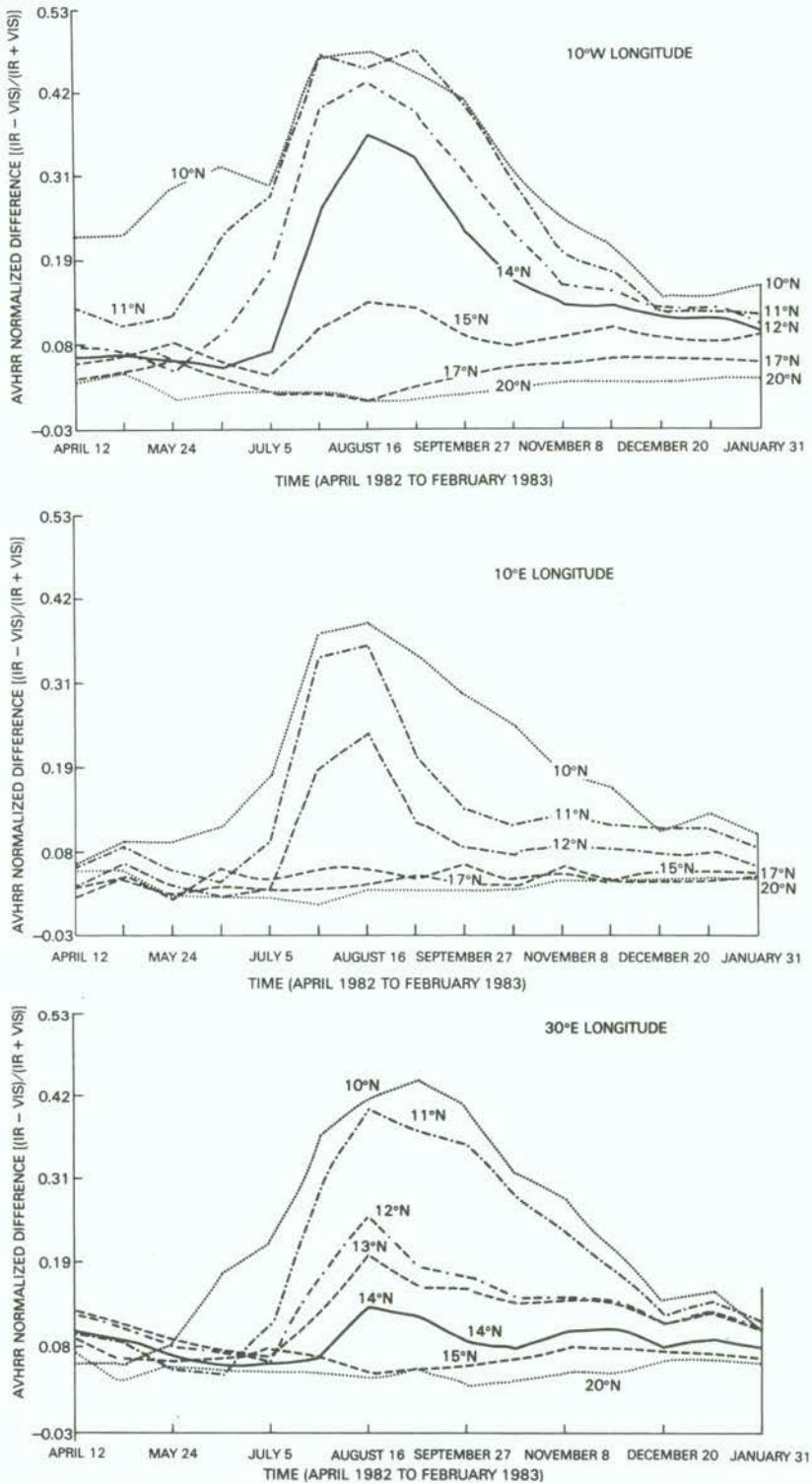
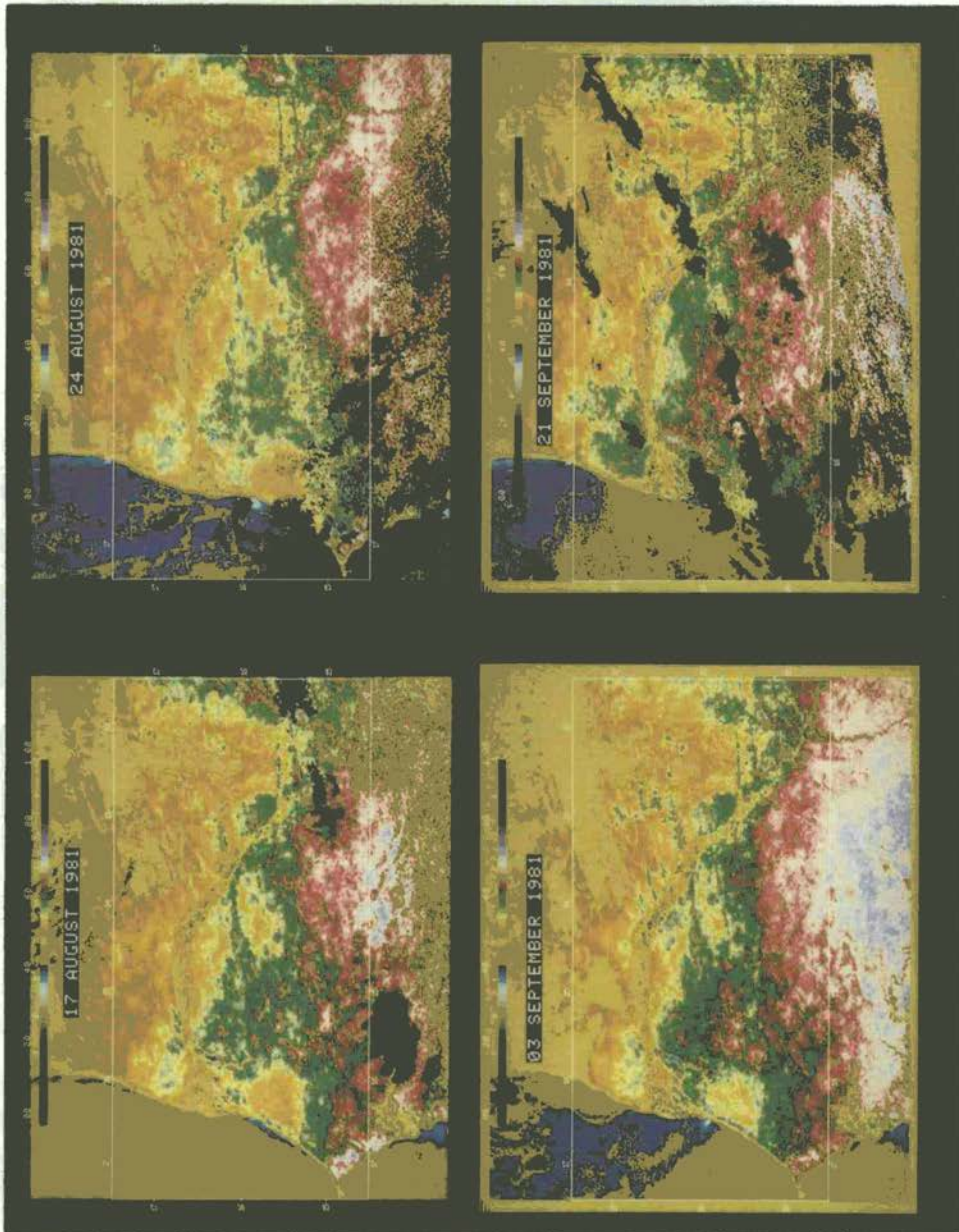


Figure 9. Spectral-temporal NDVI plots for three N-S transects across the Sahelian Zone at 10°W, 10°E and 30°E from April 1982 to February 1983.



(a)

Figure 10. Full resolution LAC images and integrated image for the Ferlo Region, Senegal for the 1981 rainy season.

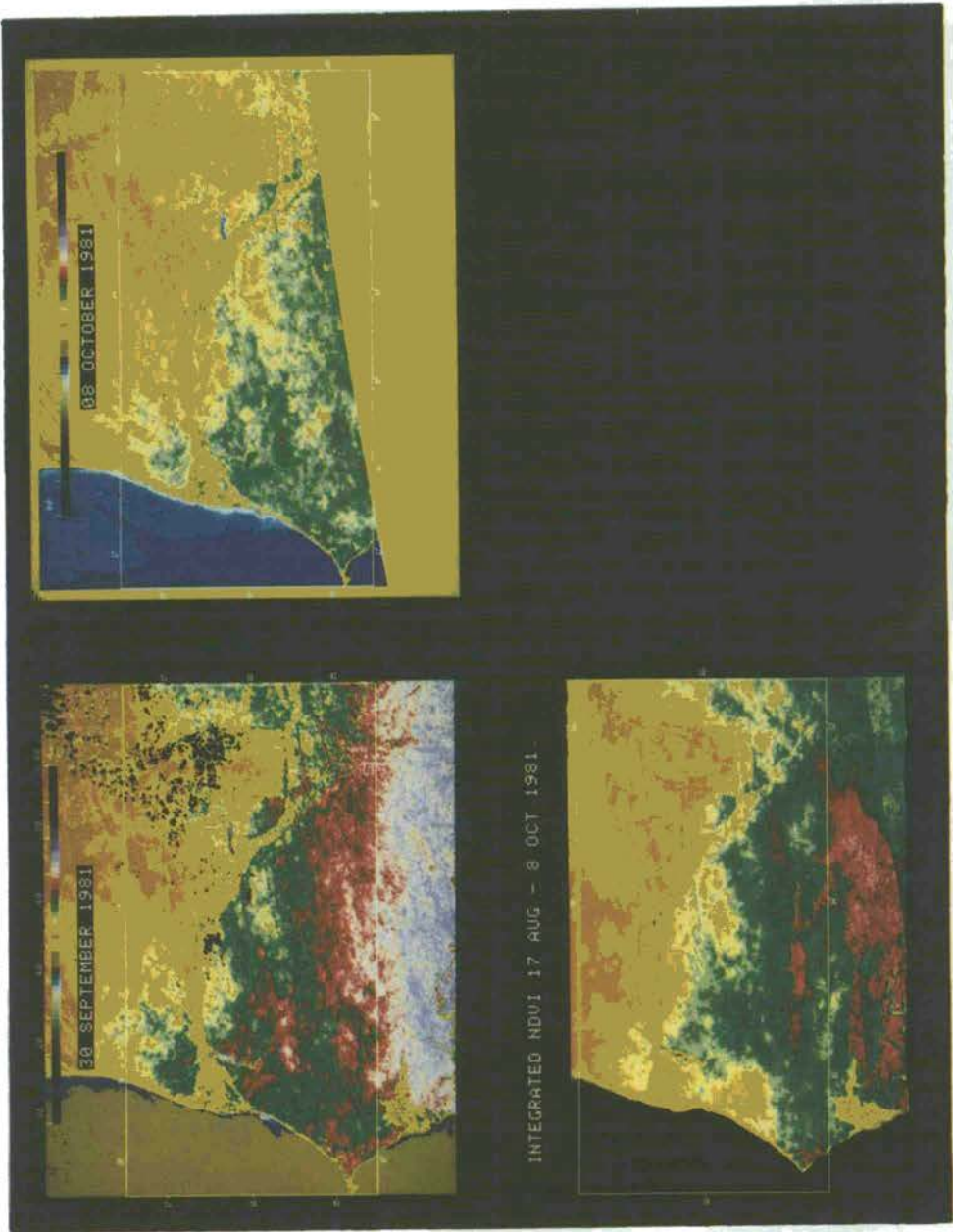


Figure 10 (b).

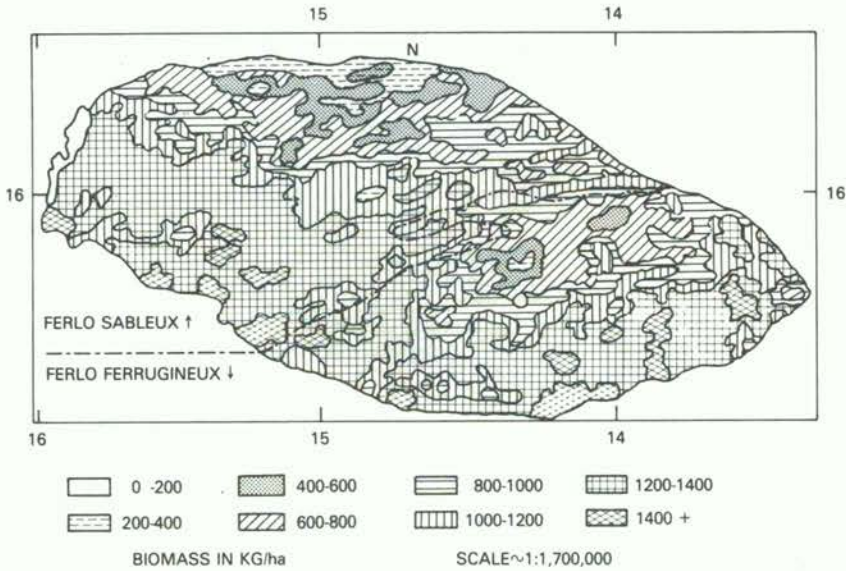
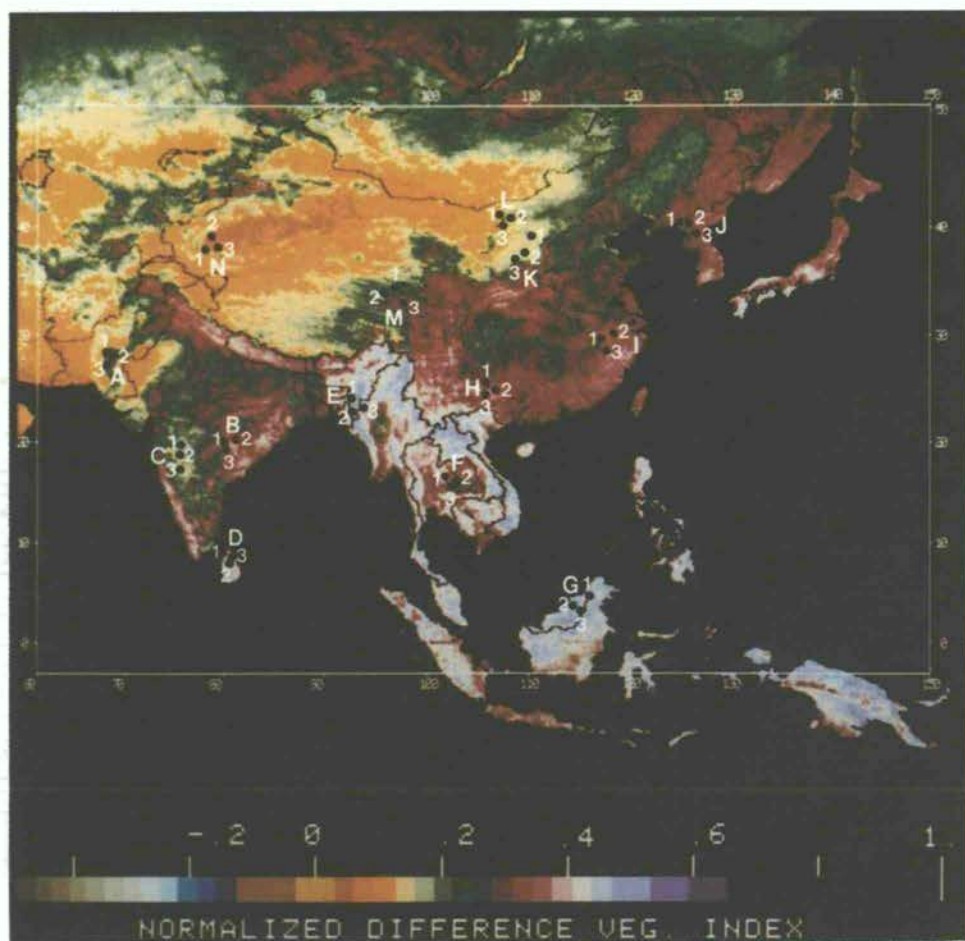


Figure 11. Preliminary map of total dry biomass for the Ferlo Region Senegal, derived from (1981) AVHRR LAC data by extrapolation from sample ground measurements (from Tucker 1983).

5. South Asian phytophenology

5.1. Spectral characterization of vegetation types

To demonstrate further the utility of AVHRR data for monitoring vegetation status at a continental scale, selected temporal plots are selected and analysed for the south Asian subcontinent. NDVI values obtained from the NOAA global vegetation index product for 15 major cover types from south-east Asia are plotted in figure 12 for thirteen 4-week compositing periods between 12 April 1982 and 28 March 1983. The locations from which the data were extracted are shown on the integrated image created for the same annual period (figure 12 (a)). Three sites were selected for each cover type to give an indication of the internal variation of the NDVI response of the cover type. For each location the average NDVI value from a 3×3 pixel array was plotted for the 13 compositing periods (figure 12 (b)). Comparison of the curves for the different cover types shows a wide range of characteristics for their temporal NDVI response. For example, the desert locations (plot N) have low NDVI values throughout the year. The semidesert grassland sites (plot K) have a small peak from August to September associated with the short growing period of the summer rains. The dry thorn forest and rough grazing land sites (plot C) have a period of low photosynthetic activity from February to July which is then followed by a gradual increase, as shown by a rise in the NDVI until November and December. A similar unimodal pattern with a slight shift in the period of maximum NDVI to September and October can be seen for the open forest and dry scrub sites in Thailand (plot F). Agricultural sites are characterized by a marked peak to the NDVI curve (plots M, L, I and A), the number, amplitude and duration of the peaks depending on such factors as the length of growing season, cropping pattern and irrigation practices. For example, plot A shows a relatively low NDVI from April to July with a marked peak in September followed by a second peak in February. This bimodal distribution

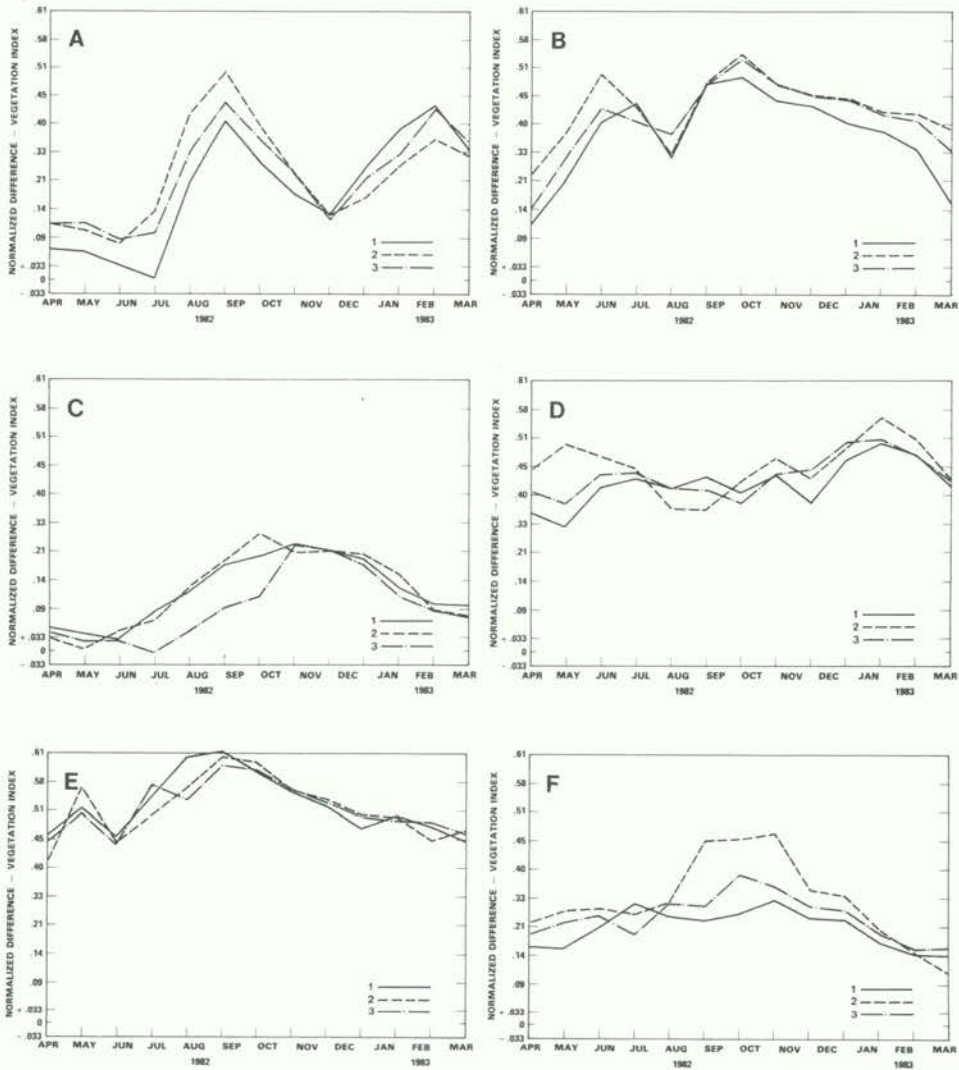


(a)

Figure 12. (a) An annual integrated image (1982–1983) showing the location of the sites used in producing the spectral-temporal plots of figure 12 (b). (b) Spectral-temporal plots of selected south east Asian cover types (1982–1983).

is associated with a double cropping pattern; a main rice crop followed by an irrigated wheat crop. The mixed forest and agriculture sites in North Korea (plot J) have a high NDVI between April and November with low values from December to February. The spring wheat and barley planted in these areas emerge following the melt of the snows in April. The snows fall in December and contribute to the period of low NDVI values. The deciduous forest sites (plot B) have a distinctive peak in September with a minimum in April. Sites with higher vegetation indices are associated with higher biomass (plots E, F and G). The tropical rain forest (plot G) has a high NDVI throughout the year with no marked peak or trough.

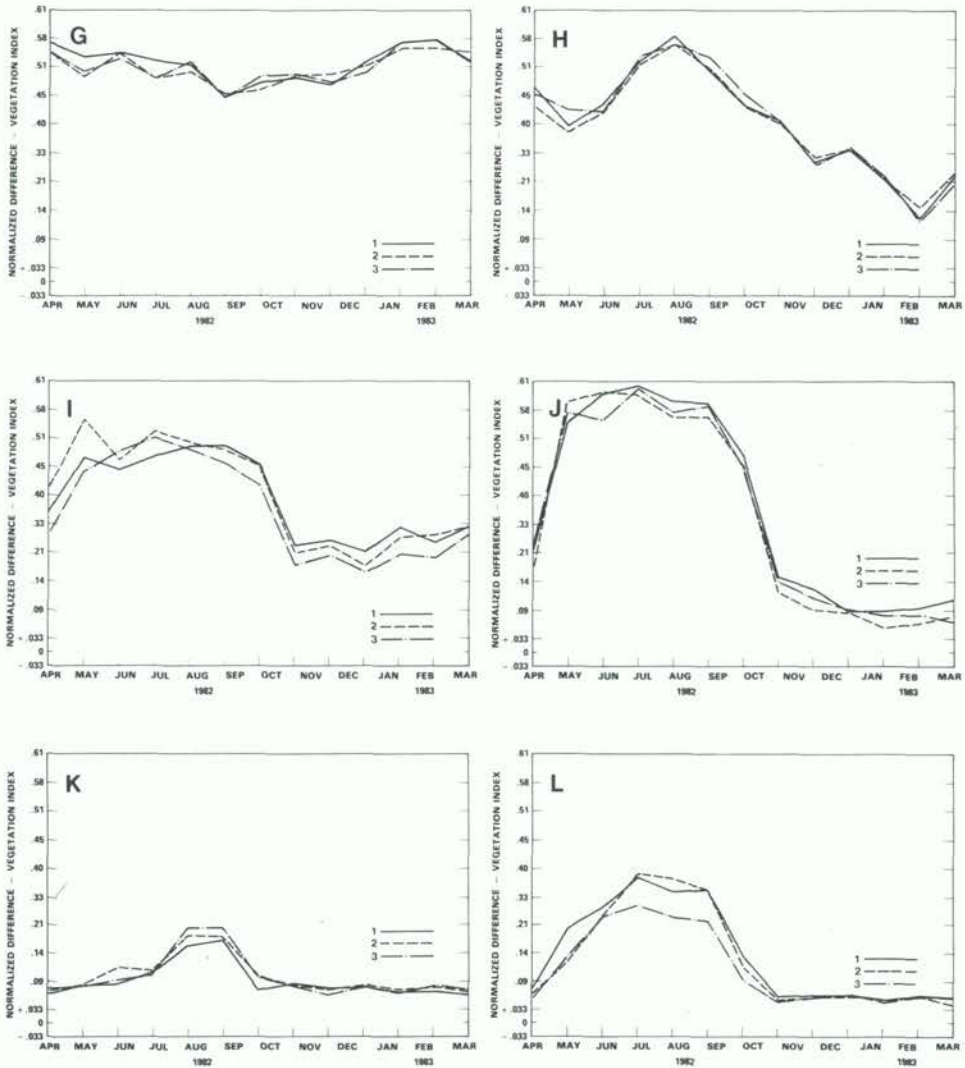
From these preliminary analyses it is apparent that different cover types exhibit characteristic NDVI curves. For natural vegetation types it is possible to trace their seasonality, to establish the timing of 'green-up' and 'senescence' and estimate the



(b)

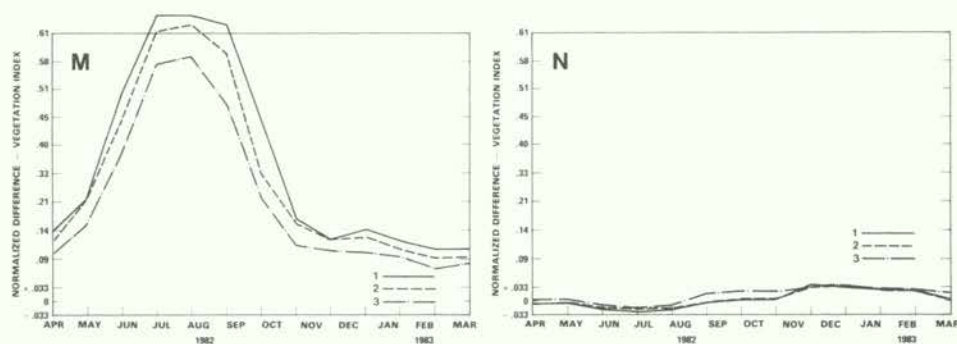
length of growing season year by year. For agricultural areas it is possible to monitor the crop development through the growing period.

Comparison of the curves from two continents (figures 2(b) and 12(b)) reveals similarities between the curve characteristics for several types, e.g. desert and rain forest, though characteristics of cover types from different continents will exhibit different seasonality largely controlled by regional bioclimatic factors. For the similarities and differences between the NDVI characteristics of the major vegetation formations to be more clearly understood, it is necessary to characterize the curves in a quantitative manner. The integrated value represents one such measure. This integrated value has been correlated with the end of season net productivity for grasslands (Tucker *et al.* 1983), but care should be taken when interpreting these values for other cover types. The integrated values are given for both continental sample sites in table 2 and are ranked by decreasing value. Although direct



(b)

comparison cannot be made between the two sets of values due to the slightly different compositing periods used, the integrated values for both continents show a general progression from desert steppe, open forest, xerophilous scrub and savanna to deciduous forest and tropical forest, with the various agricultural sites being distributed throughout the range. This ranking appears to show a general order associated with increasing green-leaf biomass. The GIMMS group is currently examining the relationship between the integrated NDVI of major vegetation formations and their net primary productivity (NPP). Use of the annual integrated value alone is inadequate to characterize the spectral curves fully; measures of their phase and amplitude need to be developed as part of a more comprehensive characterization of the curves.



- A – Irrigated Agriculture (wheat, rice), Khairpur, West Pakistan
- B – Deciduous Forest, Madhya Pradesh, India
- C – Thorn Forest and Rough Grazing Land, Deccan Plateau, India
- D – Secondary Scrub Forest, Northern Province, Sri Lanka
- E – Tropical Evergreen Forest, Chin State, Burma
- F – Open Forest and Xerophilous Scrub, Khorat Plateau, Thailand
- G – Tropical Rain Forest, Pensiangari, North Borneo
- H – Agriculture (2 crops; rice and wheat), Kweichow Province, China
- I – Agriculture (rice and winter wheat), Anwei Province, China
- J – Mixed Forest with Agriculture, Northern Interior, North Korea
- K – Semi-Desert Grassland, North Shenshi Province, China
- L – Irrigated Agriculture (barley, koaling, rice), Wu-Yuan, Inner Mongolia
- M – Agriculture (rice), Szechuan Province, China
- N – Desert, Maral Barhi, Sinkiang, China

(b)

5.2. Seasonal cropping patterns for the agricultural areas of China

Monitoring changes in the vegetation patterns associated with agricultural areas may provide a useful input to crop simulation models and agricultural production monitoring programmes. The feasibility of monitoring cropping patterns using AVHRR data is demonstrated for selected agricultural regions of China.

NDVI values were plotted for fifteen 3-week compositing periods, i.e. from 12 April 1982 to 28 March 1983, for nine major agricultural regions of China (figure 13). The graphs show representative plots of the NDVI selected from one of five locations, each of which was selected from the centre of each region. The regions are groupings of the provinces of China and were taken from a report by the CIA (1971). Interpretation of the plots was made by reference to Nuttonson (1963), Cheng-Siang Chen (1970) and Buchanan (1970).

The plots are presented as two groups separating the predominantly wheat-growing areas to the north and the rice-growing areas to the south. This major agricultural boundary is marked on the map by a dashed line (figure 13). The NDVI curves demonstrate different phenological characteristics for these two areas; the southern rice plots (A, B and C) have two peaks and show generally smoother curves than the unimodal winter-wheat (F and G) and spring-wheat (H and I) plots. Plots D and E represent the wheat and rice regions which form a transitional boundary between the northern and southern agricultural regions.

The spring-wheat region (H) and the sorghum-*soybean* region (I) are the only farming areas in China where no winter crops can be planted due to low temperatures. Crops are planted in the spring or early summer (April and May) and harvested in August or September. These regions are characterized by one crop a

Table 2. Ranked integrated annual NDVI values from the global vegetation index product for selected cover types for South American and south-east Asia.

South America				South-east Asia			
Location	Cover type	Integrated value	\bar{x}	Location	Cover type	Integrated value	\bar{x}
C	Tropical seasonal forest	0.388	0.391	E	Tropical evergreen forest	0.376	0.373
		0.393				0.367	
		0.391				0.376	
N	Tropical forest	0.405	0.383	G	Tropical rain forest	0.376	0.372
		0.366				0.365	
		0.377				0.375	
F	Coastal forest	0.360	0.353	D	Agriculture	0.312	0.319
		0.343				0.327	
		0.355				0.317	
H	Humid pampas	0.358	0.348	H	Agriculture	0.294	0.219
		0.351				0.283	
		0.334				0.296	
B	Tropical rain forest	0.357	0.345	B	Deciduous forest	0.272	0.284
		0.325				0.311	
		0.355				0.269	
G	Mixed agriculture and forest	0.304	0.327	I	Agriculture	0.274	0.279
		0.326				0.289	
		0.352				0.274	
E	Woody savanna	0.326	0.324	M	Agriculture	0.270	0.246
		0.311				0.253	
		0.335				0.216	
D	Scrub and thorn woodland	0.234	0.234	J	Mixed forest and agriculture	0.251	0.245
		0.209				0.250	
		0.335				0.233	
A	Savanna	0.246	0.223	F	Open forest	0.191	0.206
		0.208				0.219	
		0.216				0.207	
J	Dry pampas	0.218	0.219	A	Irrigated agriculture	0.194	0.201
		0.239				0.211	
		0.200				0.210	
L	Arid steppe	0.131	0.132	L	Irrigated agriculture	0.146	0.143
		0.150				0.146	
		0.116				0.137	
I	Steppe	0.092	0.125	K	Semi-desert grassland	0.110	0.114
		0.121				0.119	
		0.161				0.113	
K	Wooded steppe	0.089	0.103	N	Desert	0.049	0.049
		0.119				0.046	
		0.104				0.053	
M	Coastal desert	0.086	0.091				
		0.113					
		0.076					

year. The NDVI follows this pattern showing a marked period of photosynthetic inactivity from October to April, increasing to a peak in August and September.

Plots G and F represent the winter-wheat regions in which wheat is planted between September and October, lies dormant until the late winter and is harvested during late May or June. There is a wide variation in the cropping patterns from west

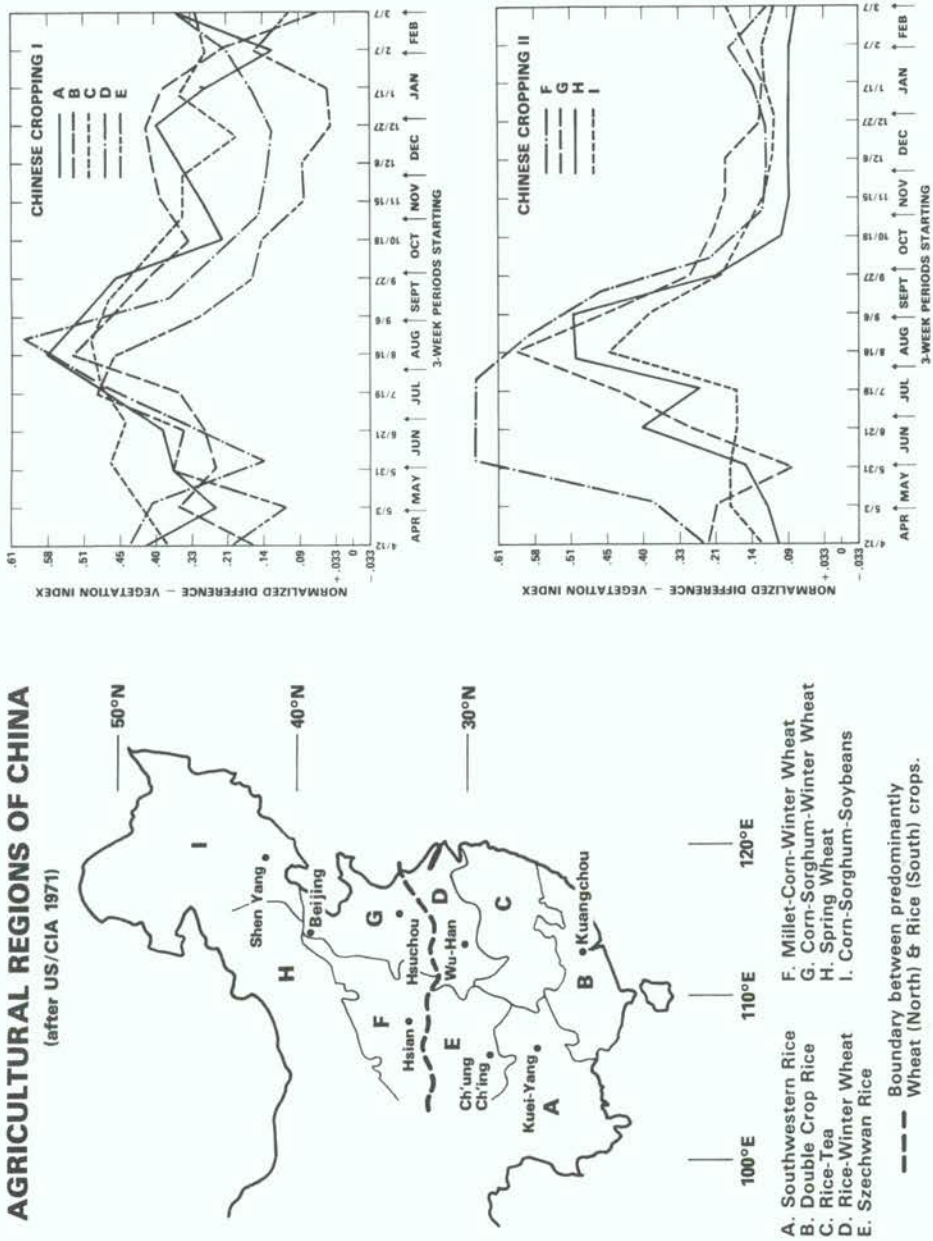


Figure 13. Spectral-temporal plots for the major agricultural regions of China (1982-1983).

to east across these two regions depending mainly on crop type and time of planting of summer crops. Three harvests in 2 years is not uncommon in these areas. Plot G follows a similar pattern to plots H and I, whereas plot F shows an earlier green-up and longer maximum period. Both plots G and F exhibit a decrease in NDVI in August and September revealing the presence of green vegetation after the wheat harvest. Although interplanting is common in these areas (Nuttonson 1963) it would be unwise to interpret these curves further without more specific ground information.

Plots E and D represent the Szechwan rice and Yangtze rice-wheat areas, respectively, and occupy the transitional zone between the wheat and rice regions represented by plots F to I and A, B and C, respectively. Rice is the major summer crop and wheat is the major winter crop often being interplanted with leguminous crops. The rice crop is sown between April and May and harvested in August and September. The wheat crop is planted in October and November and is harvested in April and May. Plots D and E are bimodal with peaks between July-August and February-March and with low values between September and January which correspond to the double cropping pattern.

The three rice regions (A, B and C) occur south of the Yangtze river in the tropical and subtropical climatic regions which are largely unsuitable for wheat production. There is considerable variation in the timing and number of crops across these rice-producing regions but three distinct areas can be delineated (Nuttonson 1963). Plot A represents the south-western rice area where double cropping has become firmly established in the high-yield basin areas and is gradually spreading. The summer crop is planted in April and May and harvested in August and September. The autumn crop is planted in September and October and is harvested in May and June. The NDVI plot representing this region is bimodal with peaks in July-August and December-January; the plot indicates a possible third peak in March-April but further AVHRR data is required for 1983 before this can be confirmed.

Plot B represents the 'double-cropping area' delineated by Nuttonson (1963), which includes some of the most intensively cultivated land in the world. Both the provinces contained by this region also include some areas of triple cropping. The corresponding NDVI plot shows a trimodal distribution with major peaks in July and December and a smaller peak in April, with a consistently high index throughout the year except for a sharp decrease in January and February. There is a difference between the April 1982 and March 1983 values which cannot be interpreted without additional data for April and May of 1983.

Plot C represents the rice-tea region where in places double and some triple rice cropping is implemented in a similar fashion to that described for plot B. The tea crop is harvested several times throughout the year and the winter crops including winter wheat are planted in October and harvested in May. The NDVI shows a peak in August associated with the main rice crop and consistently high values through to February.

From this preliminary study of 1 year of data, a good correspondence can be established between the NDVI patterns and vegetation status as interpreted from general descriptions of the regional agricultural cropping patterns. Further analysis is required for specific locations relating crop phenology and status to the temporal variation of the vegetation indices to assess quantitatively the precise nature of this relationship.

5.3. Multitemporal analysis of Indian forest types

Up-to-date estimates of the areal extent of major forest types and quantitative information on their phenology are lacking for large areas of southern Asia. The AVHRR sensors may provide an additional source of data to supplement existing forest inventory procedures. In the following example AVHRR data are used to monitor the seasonality of selected Indian forest types for a 1 year period.

Vegetation indices were plotted for fifteen 3-week compositing periods between 12 April 1982 and 28 March 1983 from fifteen representative sites for four major Indian forest types. The sites were located using broad forest-cover-type maps at 1:2 000 000 and 1:4 500 000 made available by the Forest Survey of India and by reference to the classic work on Indian forests by Champion and Seth (1968). Four NDVI plots were produced for each of the selected locations for the different forest types and a typical curve was chosen to represent each of the locations. The plots are presented in figure 14 along with the location of the sample sites.

Tropical wet evergreen forest is represented by plot 1. Sites 1 and 2 represent the southern wet evergreen forest, specifically the west coast forest type described by Champion and Seth (1968). Sites 3 and 4 represent the northern tropical wet evergreen forest of the Assam type. These forest types are virtually identical consisting of tall dense multilayered evergreen canopies. The NDVI plots for these two types are similar in their general pattern showing a peak in August and September with the lowest values occurring in January and February. These tropical forest sites are characterized by generally high NDVI values throughout the year. The marked drop in value for the west-coast plots for one 3 week period in July is caused by persistent cloud cover. In fact, most of the plots exhibit a marked decrease in June and July which is almost certainly due to cloud contamination of the NDVI values at this time which corresponds to the beginning of the cloudy monsoon period (Subbaramaya *et al.* 1982). Further examination is currently being performed at GSFC to develop optimum procedures for minimizing the effects of clouds and for identifying cloud-contaminated pixels.

In the Himalayan moist temperate forest (figure 14) sample sites were selected for locations in Jammu and Kashmir and consist of temperate broadleaved oak and coniferous forests. This forest type extends along the length of the Himalayas between the subtropical forests and the subalpine forests. The vegetation index plots for the selected sites show a period of maximum NDVI in the summer and a minimum period in March–April during the dry season. This corresponds to the leafless period for the deciduous species in the Himalayas.

The tropical dry deciduous forest class includes the southern tropical dry deciduous and the dry teak forest types. These forest types are usually leafless for several months during the dry season and the understory is commonly deciduous consisting of shrubs or grasses. Most of the tree species can be found in the moist deciduous forests where they are better developed. The NDVI plots for this forest type are taken from four widely dispersed locations. All the plots show relatively low values from April to June increasing to high values for August and September. The NDVI values remain high until there is a gradual decrease in the green vegetation cover starting in December.

The sample sites for tropical moist deciduous forest were taken from Madhya Pradesh in central India. The chief feature of the moist deciduous forest is a leafless period during the dry season, generally in March and April, although evergreen species may occur in the understorey. In the areas represented by the plots (figure 14)

SELECTED INDIAN FOREST TYPES

[After Champion and Seth 1968]

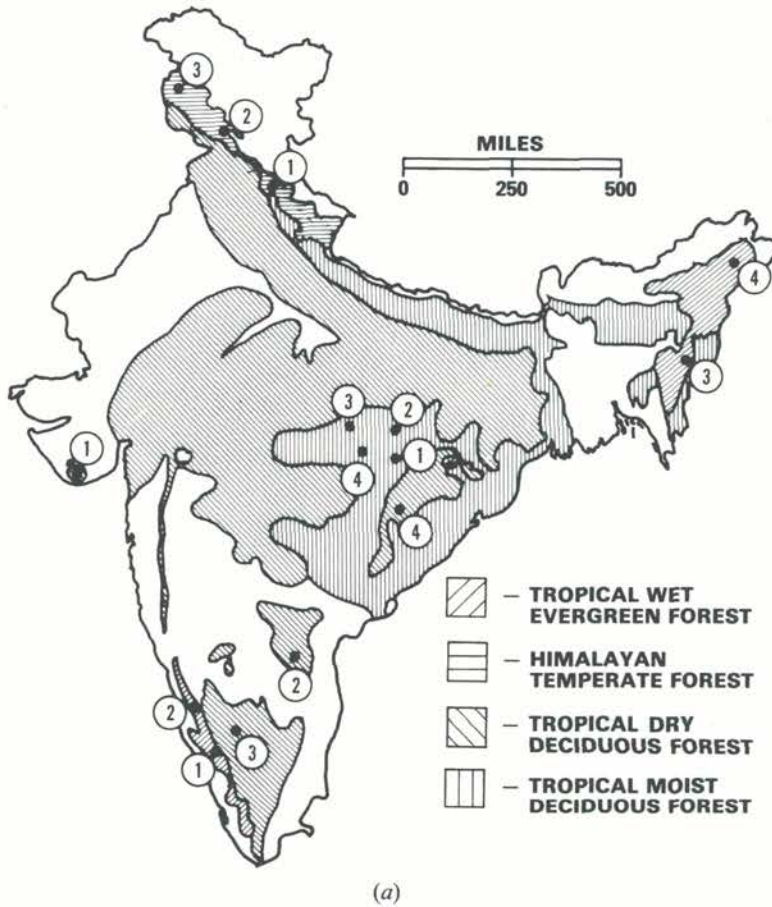
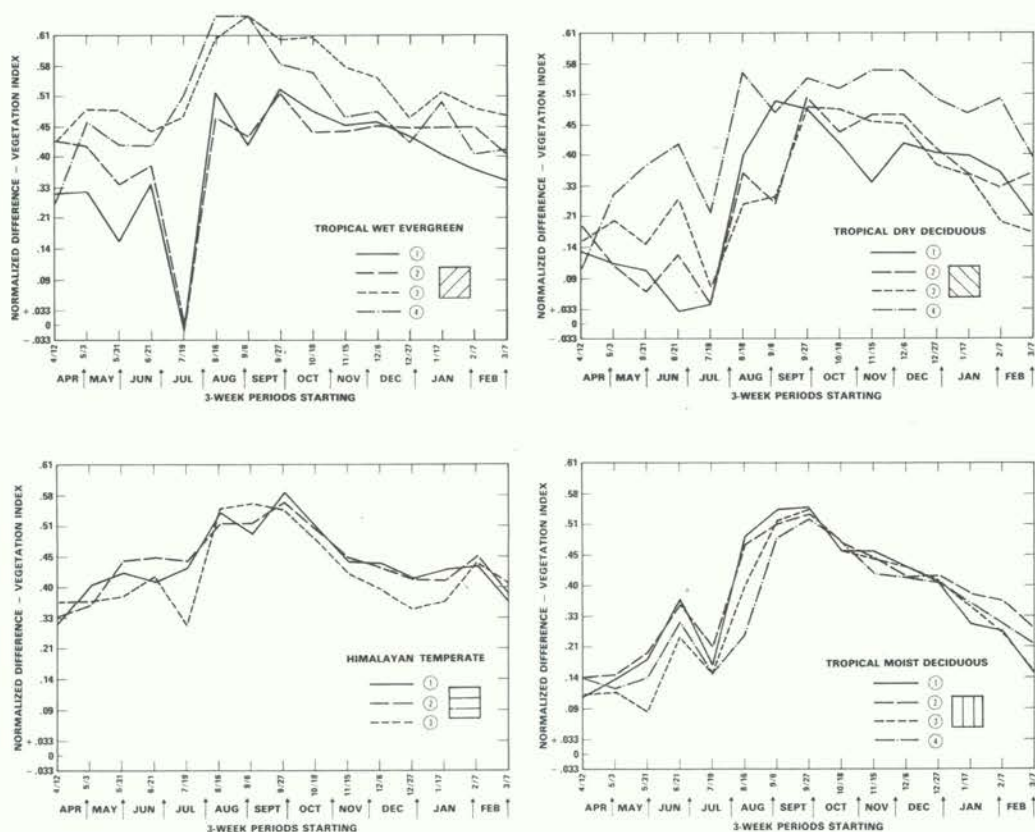


Figure 14. (a) The location of the sites used in producing the spectral-temporal plots of (b). (b) Spectral-temporal plots for selected Indian forest types (1982–1983).

there is a mixture of both southern and northern moist deciduous forest subgroups described by Champion and Seth (1968). The NDVI plots for the moist deciduous forest (figure 14) show a maximum value in September and October, associated with the full-leaf period at the end of the rainy season. The amount of green-leaf cover decreases from February to April associated with a leafless dry period and is represented by low NDVI values.

The northern moist deciduous forest includes the moist peninsular Sal forest (*Shorea* sp.) which is effectively semi-evergreen with a leafless period of between 10 and 15 days (Champion and Seth 1968). The delineation of such evergreen forests can be clearly made by comparing November (full leaf) and March (leafless) imagery. As an example, the NDVI images derived from AVHRR LAC data for 9 November 1981 and 18 March 1982 for the Satpura Range and the Wainganga Plain of Madhya Pradesh are shown in figure 15. The semi-evergreen sal forests can be clearly distinguished in the dry-period image (March) by the red and green colour



(b)

coding. The extent of the deciduous forest which includes moist deciduous teak-bearing forests, southern moist mixed forest and southern dry deciduous forest types, corresponds approximately to the high vegetation index values (purple colours) in the full-leaf period image (November). A joint study is currently underway with the UN/FAO Forestry Department and the Forest Survey of India to evaluate quantitatively the utility of the AVHRR LAC data for such forest-type discrimination and to compare the results with those obtained from LANDSAT MSS imagery. The preliminary results show that for forest-non-forest discrimination in areas of low relief at 1:1 000 000 the AVHRR LAC data provide results comparable with those from LANDSAT MSS and that selected two-date imagery permits evergreen and deciduous forest discrimination. An example of data being used in this pilot evaluation project is presented in figure 16 and provides a visual comparison of a full-frame LANDSAT MSS colour composite and the equivalent area of an AVHRR LAC pseudo-colour composite for forest-non-forest delineation. The pseudo-colour composite simulates the conventional MSS colour composite and was derived by contrast enhancement of LAC channels 1 and 2, assigning blue and green colours to channel 1 and red to channel 2.

5.4. Examination of vegetation/climate response using AVHRR data

The distribution of natural vegetation formations has been closely linked to controlling environmental parameters. For example, on the basis of the selected

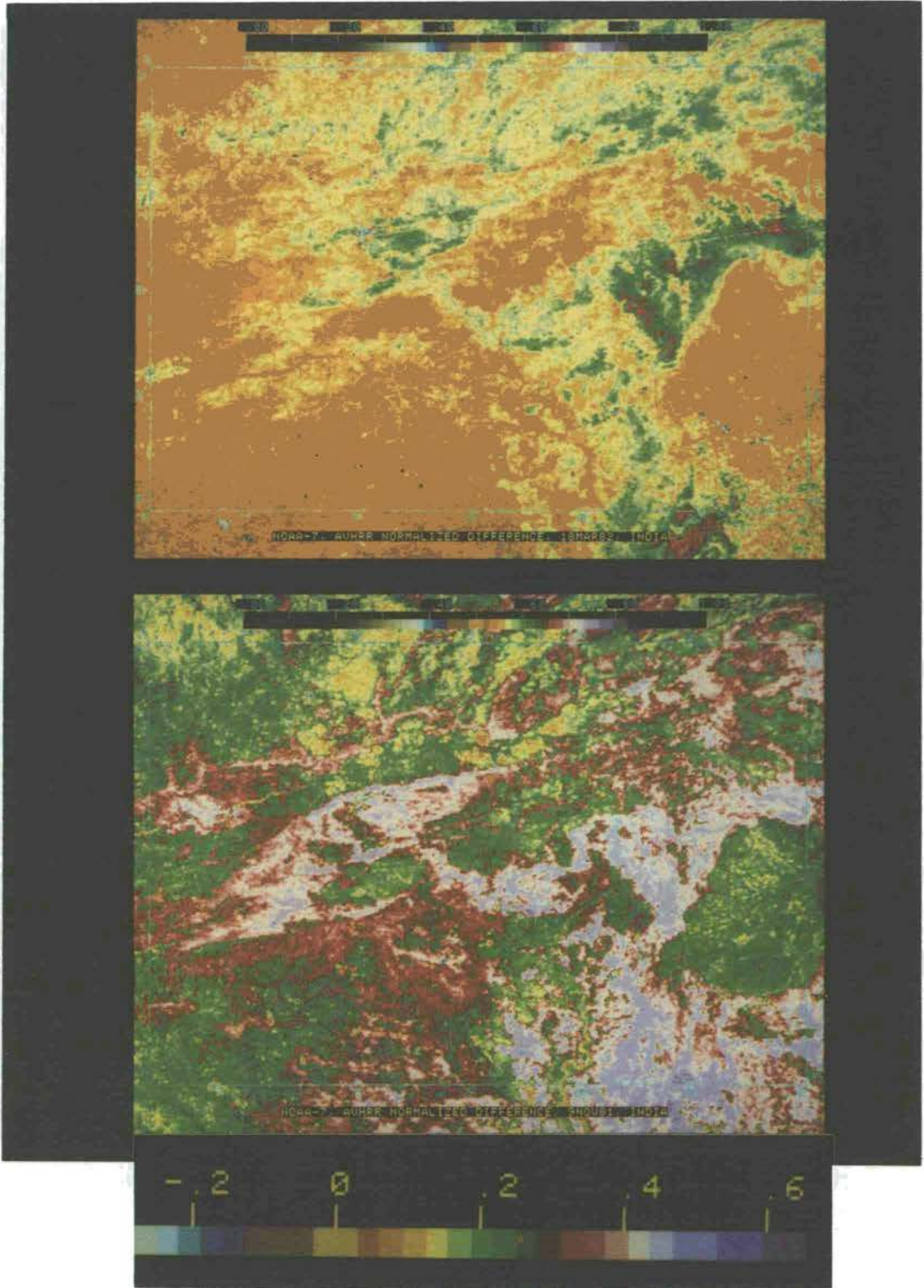


Figure 15. LAC NDVI images from November 1981 and March 1982 for Madhya Pradesh, India.

**AVHRR(LAC)/LANDSAT(MSS) COMPARISON
KATMANDU, NEPAL**



**NOAA-7—AVHRR LAC DATA (Ch 1, 2)
1 km RESOLUTION (1.5x ENLARGEMENT)
NOVEMBER 27, 1981**



**LANDSAT-3—MSS DATA (Ch 4, 5, 7)
80m RESOLUTION (FULL FRAME)
NOVEMBER 11, 1981**

Figure 16. A comparison of AVHRR LAC and LANDSAT MSS false color composites of Katmandu, Nepal for November 1981.

parameters of mean annual rainfall, temperature and potential evapotranspiration (PET), Holdridge (1947) produced a simple model for the occurrence of major vegetation formations. Similarly, agrometeorological studies have used the relationship between crop growth and environmental factors to identify agricultural limits, estimate cropping potential and to forecast crop yield (Frere and Popov 1979, Oldeman and Frere 1982). Quantitative information on the distribution of the major vegetation formations and their seasonal variations derived from AVHRR data may provide a means to test and examine these relationships and further develop such models.

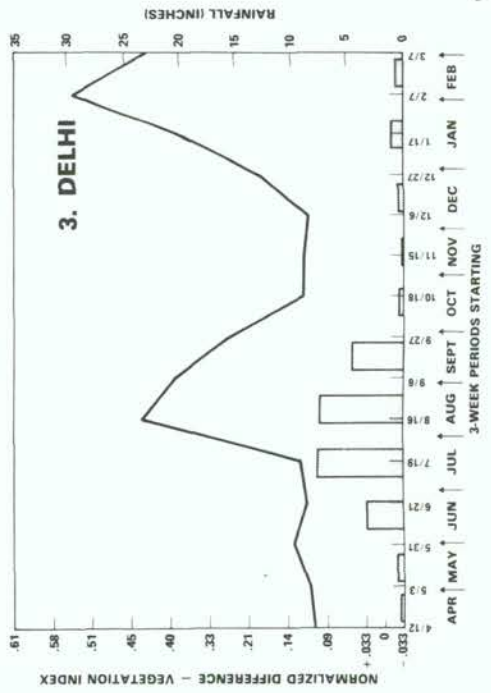
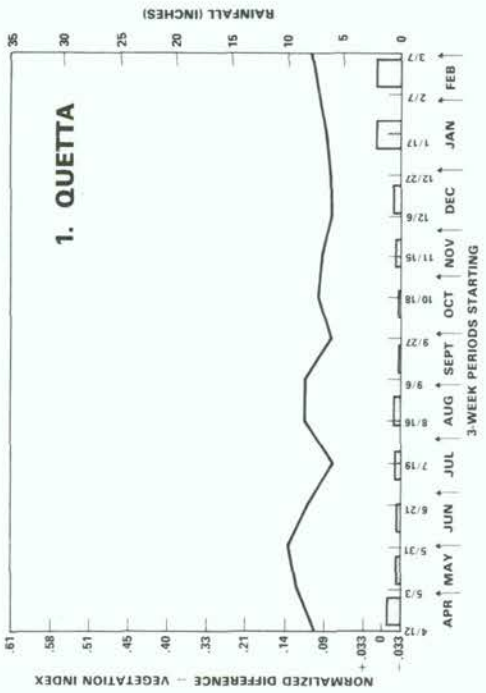
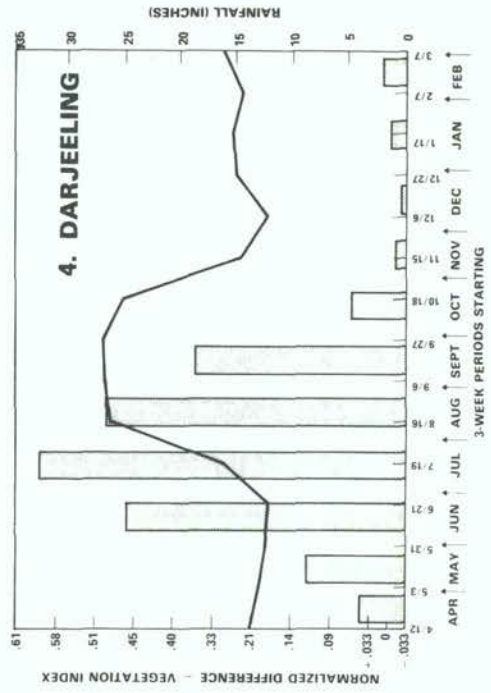
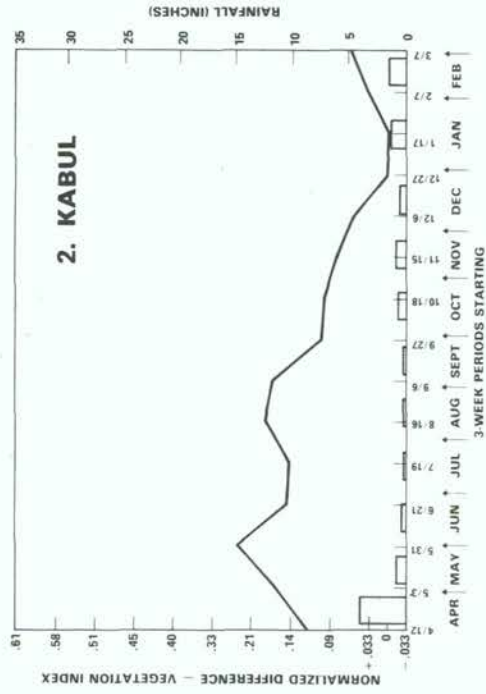
As a first step in establishing the relationships between the normalized difference vegetation index and environmental factors, we have plotted mean monthly rainfall against the NDVI for the 1982–1983 period, for selected climatic stations representing different climatic zones as defined by Trewartha (1968). The climatic data associated with each station were extracted from two main sources (Tanner 1964, Muller 1982) and are presented in table 3. The NDVI data were extracted for a 40 km × 40 km (2 × 2 pixels) sample from the approximate location of the climate station and are plotted with the mean monthly rainfall for the monitoring period (figure 17).

It should be noted, however, that only general relationships can be established between vegetation and rainfall for these plots, as mean monthly rainfall calculated over several years is being compared with actual vegetation indices for a 1 year period. Examination of the plots shows similar patterns between rainfall and NDVI but reveals a distinct phase shift between the rainfall and the vegetation index plot, which is due to a lag between the periods of rainfall and the resultant vegetation growth. A similar relationship for North American vegetation is shown by Goward *et al.* (1985). The plot for Quetta (figure 17.1) shows both low rainfall and vegetation index readings throughout the year. The plot for Darjeeling (figure 17.5) shows a generally high rainfall and high vegetation index with a considerable range in both values during the year. The plots for Pontianak (figure 17.7) show relatively high overall values with a small range. Several of the more important climatic parameters from the selected stations are listed in table 3 for comparison with the integrated NDVI. No statistical correlations have been derived because of the small number of samples; however, examination of the figures suggests some interesting conclusions. The limitations of the potential evapotranspiration (PET) as an indicator of vegetation occurrence and productivity can be seen. There is a general positive correlation between PET and the NDVI values (e.g. plots 1 and 7) but there are exceptions such as where the potential for vegetation growth is low and the mean monthly NDVI is relatively high (Darjeeling plot 4). In this instance the controlling factor is likely to be temperature which is relatively low at this high elevation site. In addition to these natural factors the human impact on vegetation status must be considered. For example, plot 3 for Delhi shows a unimodal rainfall distribution and a bimodal vegetation distribution. This is an agricultural area with a double-cropping pattern, the rice or maize crop rely on the summer rains for growth, whereas the preceding wheat crop is irrigated, hence producing the bimodal NDVI distribution.

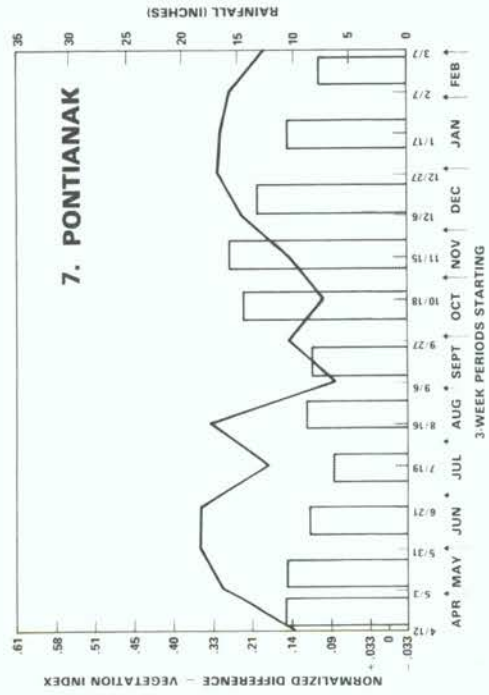
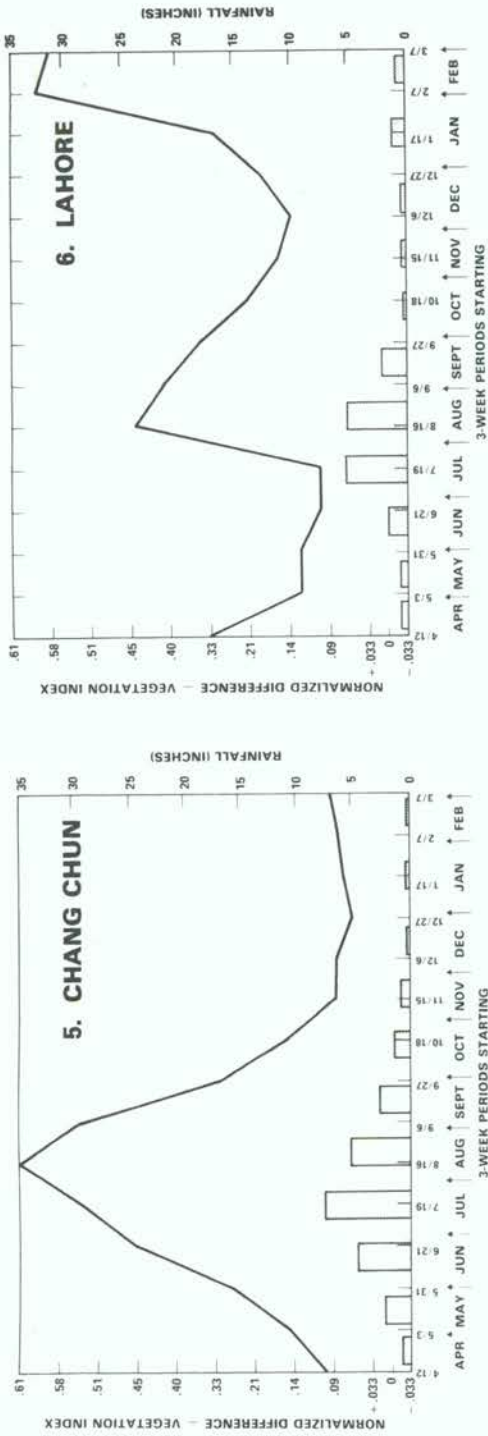
From this cursory comparison of rainfall, climate indicators and vegetation index through the year it is clear that information derived from the NDVI provides us with a tool to examine the relationships between vegetation distribution and status during the growing season and the controlling environmental factors. In addition, the

Table 3. Integrated annual NDVI and climate statistics for selected stations in south-east Asia.

Plot	Station	Lat. (N)	Long. (E)	Elevation (ft)	Climate class	Mean temp. (°F)	Ann. temp. range (°F)	Total rainfall (in)	Potential E.T.	Annual integrated NDVI
1	Quetta	30.25	67.0	5500	BWh	58	38	10	822	0.119
2	Kabul	34.50	69.17	6000	Csa(Hd)	54	49	13	730	0.143
3	Delhi	43.83	77.23	718	Caw	78	34	28	1469	0.204
4	Darjeeling	28.66	88.33	7400	Cwb(Hc)	53	32	123	655	0.279
5	Chang Chun	31.55	125.33	704	Dw	40	74	24	634	0.185
6	Lahore	27.03	31.55	642	Bahw.	75	38	20	1361	0.235
7	Pontianak	0.08	109.27	6	Af.	79	2	126	1668	0.360



(a)



(b)

Figure 17. Plots of AVHRR NDVI values (April 1982 to February 1983) and mean monthly rainfall data for selected Southeast Asian climate stations.

vegetation distribution as derived from the satellite imagery provides a means by which existing climate-based models of vegetation-formation distribution may be tested.

6. Summary and conclusions

The previous examples of imagery from three continents demonstrate that the AVHRR system provides us with a tool with which we can monitor the seasonal dynamics of the world's vegetation at a range of scales. Through the daily coverage of the AVHRR system combined with temporal compositing of the NDVI we can obtain essentially cloud-free imagery for the entire land surface of the Earth on a regular and timely basis. The NDVI has been shown to be related to green-leaf activity and as such provides a useful means by which to monitor vegetation phenology.

At the coarsest resolution of 15 km the resampled GVI product provides both a unique perspective and quantitative information on vegetation dynamics at a global scale. The distribution of the major vegetation formations and their seasonal variations as portrayed by the NDVI for a 1 year period are discussed within the text of this paper. At the finest resolution, the 1 km LAC data product can be used to monitor vegetation dynamics at a regional scale (1:1 000 000) comparable with that available from the LANDSAT system. A comparison of the different levels of information available from GVI, GAC and LAC products are given for Rondonia, South America, and indicate the utility of such data as the first in a series of data-collection stages in a multilevel approach to vegetation monitoring.

Variations in the NDVI over a 1 year period are shown to be related to the known phenology of sample cover types for South America and south-east Asia. The 8 km African NDVI product is used to analyse seasonal variations between four monthly periods and to show the potential of the data for drought monitoring.

Examples of the GVI data are given for the study of the seasonal dynamics of Chinese cropping patterns and Indian forest types and show the potential practical applications of such a product. Finally, a comparison of vegetation status as portrayed by the GVI data and generalized climatic data is made for selected south-east Asian sites to suggest the utility of the data for developing ecological models.

Although the AVHRR NDVI data provide us with a novel means by which to quantify vegetation dynamics and to suggest a large number of potential applications, we must be aware of the limitations inherent in this data source. For example, overestimation of the presence of vegetation in certain conditions is possible through the compositing and by the way in which the GAC data are derived from the LAC data by the present NOAA resampling technique. It is clear that at such coarse spatial resolutions each pixel represents a complex range in surface conditions which contribute to the signal received by the satellite. This complexity makes interpretation of the contribution of the components to the signal difficult at the pixel level. When viewed over time the contribution of these different surface components becomes even more complex to model. Furthermore, as yet there is little quantitative research on the optimum spatial and temporal frequencies for monitoring the different cover types. In addition, we have yet to overcome problems of cloud cover at certain times of the year in tropical areas and are currently developing improved cloud-masking techniques. However, for certain areas of the world with continuous cloud cover during part of the year we will be unable to overcome this limitation using multispectral sensing systems. It is also clear that

atmospheric effects although minimized by the compositing technique, will impact on the NDVI response under certain conditions and care should be taken when examining areas subject to strong atmospheric haze. Part of the present problem with analysing such coarse-resolution data is the difficulty of collecting sufficient ground data to represent the conditions over such large areas. Although the satellite data are georeferenced which enables geographical co-ordinate schemes to be applied to the data, more frequent updating of the satellite ephemeris data would lead to improved registration of the LAC data. Our future programme of planned activities include establishing international test sites to enable objective monitoring and analysis of the vegetation phenology on the ground, as observed by the AVHRR and through assessment of existing data sources and other sources of remotely sensed data. In this respect it is important to establish and preserve the necessary archival AVHRR data sets to permit interannual comparisons, enabling a clear picture of the significance of observed changes within a 1 year period to be obtained.

Although this paper has emphasized almost exclusively the role of coarse resolution sensors for vegetation monitoring we believe that the AVHRR system should be used in conjunction with high-resolution sensors and systematic ground data collection to provide the means for better management of the Earth's resources.

In conclusion, we believe that the science community now has at its disposal a new important source of data to provide quantitative information on the vegetation of our planet to answer questions which heretofore have been unanswerable due to the lack of spatially comprehensive and reliable data.

Acknowledgments

The GIMMS project is a NASA programme and we acknowledge the valuable external support from UNEP/GEMS, UN/FAO and ILCA who provided data and ground information to enable this study to be undertaken. The Sensor Evaluation Branch at NASA/GSFC, in particular, Tom Goff, Jim Gatlin and Bob Rank, were responsible for the software development and computer operations associated with this project. Personal thanks should go to Drs. K. D. Singh and S. Molhatra of UN/FAO and to Dr. Shao Xiang Ni of Reading University for consultation on certain aspects of the work. The publication of this document was possible through the financial support of UNEP/GEMS.

References

- ASHLEY, M. D., and REA, J., 1975, Seasonal vegetation differences from ERTS Imagery. *Photogramm. Engng*, **41**, 713.
- BOESCH, H., and BRUNNSCHWEILER, D., 1960, Seasonal changes of the agricultural landscape interpreted from aerial photographs. *Geographica helv.*, **15**, 257.
- BOLIN, B., 1984, Biogeochemical processes and climate modelling. In *The Role of Terrestrial Vegetation in the Global Carbon Cycle: Measurement by Remote Sensing*, edited by G. M. Woodwell (Wiley).
- BOX, E. O., 1981, Macroclimate and plant forms: an introduction to predictive modeling in phytogeography. *Tasks in Vegetation Science 1*, edited by H. Lieth (The Hague: Junk).
- BROWN, D. S., 1952, Climate in relation to deciduous fruit production in California, V. The use of temperature records to predict the time of harvest of apricots. *Proc. Am. Soc. hort. Sci.*, **60**, 197.
- BROWN, L. H., and COCHEME, H., 1973, A study of the agroclimatology of the highlands of East Africa. WMO Technical Note 125, Geneva, Switzerland, 197 pp.
- BRUNNSCHWEILER, D., 1957, Seasonal changes of agricultural pattern: a study in comparative air-photointerpretation. *Photogramm. Engng*, **23**, 131.

- BUCHANAN, K., 1970, *The Transformation of the Chinese Earth* (London: Bell).
- CARNEGIE, D. M., SCHRUMPF, B. J., and MOUAT, D. A., 1983, Rangeland applications. In *Manual of Remote Sensing*, 2nd edn, edited by R. N. Colwell (Falls Church, Virginia: American Society of Photogrammetry), p. 2325.
- CHAMPION, H. G., and SETH, S. K., 1968, *A Revised Survey of the Forest Types of India* (Delhi: Government of India Press), 600 pp.
- CHENG-SIANG CHEN, 1970, *The Agricultural Regions of China* (Silver Spring, Maryland: American Institute of Crop Ecology), 50 pp.
- CIA, 1971, *Peoples Republic of China Atlas* (Washington, D.C.: U.S. Government Printing Office), 82 pp.
- CICONE, R. C., and METZLER, M. D., 1982, Comparisons of Landsat MSS, Nimbus 7 CACS and NOAA 6/7 AVHRR sensors for land use analysis. *Proceedings of the Eighth International Symposium on Machine Processing of Remotely Sensed Data*, Purdue University, Indiana, p. 291.
- COCHEME, J., and FRANQUIN, P., 1975, An agroclimatology survey of a semiarid area in Africa south of the Sahara. WMO Technical Note, No. 86, Geneva, Switzerland, 136 pp.
- CURRAN, P. J., 1980, Multispectral remote sensing of vegetation amount. *Prog. Phys. Geogr.*, **4**, 315.
- DETHIER, B. E., 1974, Phenology satellite experiment. Final Report, NAS5-21781, Cornell University, Ithaca, New York.
- FAO, 1978, Crop calendars. FAO Plant Production and Protection Paper, No. 12, UN/FAO, Rome, 124 pp.
- FAO/UNESCO, 1971, *Soil Map of the World: South America*. Memoir (Paris: UNESCO).
- FRERE, M., and POPOV, G. F., 1979, Agrometeorological crop monitoring and forecasting. FAO Plant Protection Paper, No. 17, UN/FAO, Rome, 63 pp.
- FUNG, I., PRENTICE, K., MATTHEWS, E., LEARNER, J., and RUSSELL, G., 1983, Three dimensional tracer model study of atmospheric CO₂: response to seasonal exchanges with the terrestrial biosphere, *J. geophys. Res.*, **88**, 1281.
- GAMMON, P. T., and CARTER, V., 1979, Vegetation mapping with seasonal color infrared photographs. *Photogramm. Engng remote Sensing*, **45**, 87.
- GATLIN, J. A., SULLIVAN, R. J., and TUCKER, C. J., 1983, Monitoring global vegetation using NOAA AVHRR data. *Proceedings of the IGAARS Symposium*, San Francisco, California I, PF2, 7.1.
- GOWARD, S. N., DYE, D. G., and TUCKER, C. J., 1985, North American vegetation patterns observed by NOAA-7 AVHRR, *Vegetatio* (in the press).
- GROUZIS, M., and METHY, M., 1983, Determination radiometrique de la phytomasse herbacee en milieu sahelien: perspectives et limites. *Acta Oecol. Plant.*, **4**, 241.
- HATFIELD, J. L., 1983, Remote sensing estimates of potential and actual crop yield. *Remote Sensing Environ.*, **13**, 301.
- HOLBEN, B. N., and FRASER, R. S., 1984, Red and near infrared response to off-nadir viewing. *Int. J. remote Sensing*, **5**, 145.
- HOLBEN, B. N., and JUSTICE, C. O., 1981, An examination of spectral band ratioing to reduce the topographic effect on remotely sensed data. *Int. J. remote Sensing*, **2**, 115.
- HOLBEN, B. N., TUCKER, C. J., and FAN, C. J. 1980, Spectral assessment of soybean leaf area and leaf biomass. *Photogramm. Engng remote Sensing*, **45**, 651.
- HOLDRIDGE, L. R., 1947, Determination of world plant formations from simple climatic data. *Science, N.Y.*, **105**, 367.
- HONEY, F. R., and TAPLEY, I. J., 1981, A vegetation response model applied to range inventory using Landsat MSS data. *Proceedings of the 15th International Symposium on Remote Sensing of the Environment*, Ann Arbor, Michigan, p. 823.
- JACKSON, R. D., SLATER, P. N., and PINTER, P. J., 1983, Discrimination of growth and water stress in wheat by various vegetation indices through clear and turbid atmospheres. *Remote Sensing Environ.*, **15**, 187.
- JORDON, C. F., 1969, Derivation of leaf area index from quality of light on the forest floor. *Ecology*, **50**, 663.
- JUNG, C. E., and CZELPLAK, G., 1968, Some aspects of seasonal variation of carbon dioxide and ozone. *Tellus*, **20**, 422.
- KIDWELL, K. B., 1984, NOAA polar orbital data users guide (TIROS-N, NOAA 6, 7, 8). NOAA, NOAA National Climate Center, Washington, D.C.

- KRIEGLER, F. J., MALILA, W. A., NALEPKA, R. F., and RICHARDSON, W., 1969, Preprocessing transformations and their effects on multispectral recognition. *Proceedings of the Sixth International Symposium on Remote Sensing of the Environment*, Ann Arbor, Michigan, p. 97.
- LIETH, H., 1971, The phenological viewpoint in productivity studies. In *Productivity of Forest Ecosystems, Proceedings of the Brussels Symposium*, edited by P. Duvigneaud (Paris: UNESCO), p. 71.
- LIETH, H., 1974, *Phenology and Seasonality Modeling* (New York: Springer-Verlag), 444 pp.
- LIETH, H., and WHITTAKER, R. H. (editors), 1975, *Primary Productivity of the Biosphere* (New York: Springer-Verlag).
- MATHER, J. R., and YOSHIOKA, G. A., 1968, The role of climate in the distribution of vegetation. *Ann. Assoc. Am. Geogr.*, **58**, 29.
- MATTHEWS, E., 1983, Global vegetation and land use; new high resolution data bases for climate studies, *J. Climate appl. Met.*, **22**, 474.
- MENAUT, J. C., 1983, The vegetation of African savannas. In *Tropical Savannas, Ecosystems of the World*, Vol. 13, edited by F. Bourlier (Amsterdam: Elsevier), p. 109.
- MORAIN, S. A., 1974, Phenology and remote sensing. In *Phenology and Seasonality Modeling*, edited by H. Lieth, (New York: Springer-Verlag), p. 55.
- MYERS, V. I. (editor), 1983, Remote sensing applications in agriculture. In *Manual of Remote Sensing*, 2nd edn, edited by R. N. Colwell (Falls Church, Virginia: American Society of Photogrammetry), p. 2111.
- MULLER, J. M., 1982, *Selected Climatic Data for a Global Set of Standard Stations for Vegetation Science* (The Hague: Junk), 450 pp.
- NOAA, 1983, Global vegetation index users guide. SDS/D/NESDIS, National Climate Data Center, Washington, D.C.
- NORWINE, J., and GREGOR, D. H., 1983, Vegetation classification based on AVHRR satellite imagery. *Remote Sensing Environ.*, **13**, 69.
- NUTTONSON, M. Y., 1963, *The Physical Environment and Agriculture of Central and South China, Hong Kong and Taiwan* (Washington, D.C.: American Institute of Crop Ecology), 300 pp.
- OLDEMAN, L. R., and FRERE, M., 1982, A study of the agroclimatology of the humid tropics of Southeast Asia. FAO Technical Report, UN/FAO, Rome, 230 pp.
- OLSON, C. E., and GOOD, R. E., 1962, Seasonal changes in light reflectance from forest vegetation. *Photogramm. Engng*, **23**, 107.
- OLSON, J., and WATTS, J. A., 1982, Major world ecosystem complexes. In *Carbon Dioxide Review 1982*, edited by W. C. Clark (Oxford: Oxford University Press).
- ORMSBY, J. P., 1982, Classification of simulated and actual NOAA-6 AVHRR data for hydrologic land surface feature definition. *I.E.E.E. Trans. Geosci. remote Sensing*, **20**, 262.
- PASCALÉ, A. J., 1972, Biological and phenological observations. In *WMO Agricultural Meteorology*, No. 310, Geneva, Switzerland, p. 185.
- PODOLSKY, A. S., 1984, *New Phenology: Elements of Mathematical Forecasting in Ecology* (New York: Wiley), 504 pp.
- ROUSE, J. W., HASS, R. H., SCHELL, J. A., DEERING, D. W., and HARLAN, J. C., 1974, Monitoring the vernal advancement and retrogradation (green wave effect) of natural vegetation. Final Report, RSC 1978-4, Texas A & M University, College Station, Texas.
- SARMIENTO, G., and MONASTERIO, M., 1983, Life forms and phenology. In *Tropical Savannas, Ecosystems of the World*, Vol. 13, edited by F. Bourlier (Amsterdam: Elsevier), p. 79.
- SCHNEIDER, S. R., MCGINNIS, S. R., JR., and GATLIN, J. A., 1981, Use of NOAA/AVHRR visible and near-infrared data for land remote sensing. NOAA Technical Report, NESS 84, USDC, Washington, D.C., 48 pp.
- SCHWALB, A., 1982, The Tiros-N/NOAA-A to G satellite series. NOAA Technical Memo, NESS 95, Washington, D.C., 73 pp.
- SEATON, H. L., 1955, Scheduling plantings and predicting harvesting maturities for processing vegetables. *Food Technol.*, **9**, 202.
- STEINER, D., 1969, Time dimension for crop surveys from space. *Photogramm. Engng*, **36**, 187.
- SUBBARAMAYA, I., BHANUKUMAR, O., and BABU, S. V., 1982, The summer monsoon rains over south east Asia. WMO Report, No. 578, Geneva, Switzerland, 316.

- TANNER, G., 1964, *A Collection of Selected Climographs*. (Wisconsin: The Cartography Institute), 43 pp.
- TARPLEY, J. D., SCHNEIDER, S. R., and MONEY, R. L., 1984, Global vegetation indices from NOAA-7 meteorological satellite. *J. Climate appl. Met.*, **23**, 491.
- TAYLOR, F. G., 1974, Phenodynamics of production in a mesic deciduous forest. In *Phenology and Seasonality Modeling*, edited by H. Lieth (New York: Springer-Verlag), 237.
- TOWNSHEND, J. R. G., and TUCKER, C. J., 1984, Objective assessment of AVHRR data for land cover mapping. *Int. J. remote Sensing*, **5**, 492.
- TREWARTHA, G. T., 1968, *An Introduction to Climate*, 4th ed. (New York: McGraw-Hill), 408 pp.
- TUCKER, C. J., 1979, Red and photographic infrared linear combinations for monitoring vegetation. *Remote Sensing Environ.*, **8**, 127.
- TUCKER, C. J., GATLIN, A., and SCHNEIDER, S. R., 1984 a, Monitoring vegetation in the Nile Delta with NOAA-6 and NOAA-7 AVHRR. *Photogramm. Engng remote Sensing*, **50**, 53.
- TUCKER, C. J., HIELKEMA, J. U., and ROFFEY, J., 1985 a, Satellite remote sensing monitoring in desert locust breeding areas. *Int. J. remote Sensing* (in the press).
- TUCKER, C. J., HOLBEN, B. N., ELGIN, J. H., JR., and McMURTREY, J. E., 1981, Remote sensing of total dry matter accumulation in winter wheat. *Remote Sensing Environ.*, **11**, 171.
- TUCKER, C. J., HOLBEN, B. N., and GOFF, T. E., 1984 b, Intensive forest clearing in Rondonia, Brazil as detected by satellite remote sensing. *Remote Sensing Environ.*, **15**, 255.
- TUCKER, C. J., TOWNSHEND, J. R. G., and GOFF, T. E., 1985 b, African land cover classification using satellite data. *Science, N.Y.*, **227**, 110.
- TUCKER, C. J., VANPRAET, C., BOERWINKLE, E., and GASTON, A., 1983, Satellite remote sensing of total dry matter accumulation in the Senegalese Sahel. *Remote Sensing Environ.*, **13**, 461.
- TUCKER, C. J., VANPRAET, C. L., SHARMAN, M. J., and VAN ITTERSUM, G., 1984 c, Satellite remote sensing of total herbaceous biomass production in the Senegalese Sahel: 1980-1984. *Remote Sensing Environ.* (in the press).
- UNESCO, 1979, *Tropical Grazing Land Ecosystems* (Paris: UNESCO), 655 pp.
- UNESCO, 1980 a, *Map of the Vegetation of South America*, 1:5 000 000 (Paris: UNESCO).
- UNESCO, 1980 b, Case studies on desertification. *Natural Resources*, Vol. XVIII (Paris: UNESCO/UNEP/UNDP), 279 pp.
- VINODGRADOV, B. V., 1977, Remote sensing in ecological botany. *Remote Sensing Environ.*, **6**, 83.
- VINODGRADOV, B. V., 1981, Remote sensing and mapping of rangelands. *Soviet J. remote Sensing*, **3**, 378.
- WHITE, F., 1983, The vegetation of Africa (memoir to accompany UNESCO vegetation map of Africa). *Natural Resources Research*, vol. XX (Paris: UNESCO), 356 pp.
- WIELGOLASKI, F., 1974, Phenology in agriculture. In *Phenology and Seasonality Modeling*, edited by H. Lieth (New York: Springer-Verlag), p. 369.

GIMMS Programme

The Global Inventory, Monitoring and Modelling Studies (GIMMS) group is part of the Laboratory for Terrestrial Physics at NASA's Goddard Space Flight Center. The GIMMS project is composed of a series of international co-operative research projects using coarse spatial resolution satellite data to inventory, monitor and model vegetation conditions at regional, continental and global scales. Current research activities address: rangeland monitoring in Sahelian Africa; deforestation assessment in the Amazon Basin; continental land cover mapping; inventory of the world's deserts and assessing the role of seasonal changes in the terrestrial biosphere on the global carbon cycle.

INTERNATIONAL JOURNAL OF REMOTE SENSING
and Remote Sensing Society's News and Letters

DEL/UNEP/GEMS.

(0904)

Editor: A. P. Cracknell, Carnegie Laboratory of Physics,
Dundee DD1 4HN, UK

Consultant Editor: J. O. Thomas, Department of Physics, Imperial College, Prince
Consort Road, London SW7 2BZ, UK

News Editor and Book Review Editor: P. A. Vass, National Remote Sensing Centre,
Royal Aircraft Establishment, Farnborough GU14 6TD, UK

Letters Editor: P. J. Curran, Department of Geography, University of Sheffield,
Sheffield S10 2TN, UK

Associate Editors: S. R. Brooks, Marconi Research Centre, UK; **G. Frayse**, Joint
Research Centre for the European Communities, Italy; **R. Harris**, University of
Durham, UK; **K. Hasselmann**, Max-Planck-Institut für Meteorologie, Hamburg,
Germany; **S. Murai**, University of Tokyo, Japan; **R. K. Raney**, RADARSAT
Project Office, Canada; **V. V. Salomonson**, NASA/GSFC, USA; **H. Shimoda**, Tokai
University, Japan; **S. Tanaka**, Remote Sensing Technology Center, Japan; **J. R. G.
Townshend**, University of Reading, UK; **R. A. Vaughan**, University of Dundee, UK

The **International Journal of Remote Sensing** covers the whole field of remote sensing from the science and technology of data acquisition, the processing of the data acquired, pattern recognition and the display and interpretation of results, through to the many and varied applications of remotely sensed data.

The journal publishes scientific papers describing original work, short technical notes, scientific letters to the editor, and commissioned review papers on important topics. 1984 saw the commencement of the publication of the **Remote Sensing Society's News and Letters**, which appears quarterly and consists of News Sections and Letters from the **IJRS** together with specific Remote Sensing Society material. The **Remote Sensing Society's News and Letters** is distributed to all members of the Remote Sensing Society and provides a substantial extension of the Society's services to members and at the same time a very important new means for members and non-members to communicate their results and views speedily.

The success of **IJRS** in attracting subscribers and material for publication has been such that, launched in 1980 as a quarterly journal, it will be appearing monthly from 1985, publishing around 1800 pages per volume.

The editors welcome the submission of papers from as many sources, and on as wide a range of topics in remote sensing, as possible. In particular, the editors would like to receive more review articles and letters; more papers from France, eastern Europe and the developing countries; and more papers on the meteorological applications of remote sensing and on the observation of planets other than Earth. Notes for authors can be supplied on request. **All authors receive 50 free reprints of each paper, and there are no page charges.**

1985 subscriptions cost £145, \$320, DM650, or £49, \$98, DM220 for members of the Remote Sensing Society.

Further information, sample copies and Notes for Authors are available from the publisher.



Taylor & Francis
London and Philadelphia

Rankine Road, Basingstoke,
Hants RG24 0PR, UK
Tel: (0256) 468011. Telex: 858540